The CD33xCD123xCD70 Multispecific CD3-Engaging DARPin MP0533 Induces Selective T Cell–Mediated Killing of AML Leukemic Stem Cells

Authors

Matteo Bianchi[1], Christian Reichen[1], Amelie Croset[1], Stefanie Fischer[1], Aline Eggenschwiler[1], Yvonne Grübler[1], Rajlakshmi Marpakwar[1], Thamar Looser[1], Patricia Spitzli[1], Christel Herzog[1], Denis Villemagne[1], Dieter Schiegg[1], Liridon Abduli[1], Chloé Iss[1], Alexandra Neculcea[1], Marco Franchini[1], Tamara Lekishvili[1], Simone Ragusa[1], Christof Zitt[1], Yvonne Kaufmann[1], Alienor Auge[1], Martin Hänggi[1], Waleed Ali[1], Teresa M. Frasconi[1], Stephan Wullschleger[1], Iris Schlegel[1], Mirela Matzner[1], Ursina Luethi[2], Bernd Schlereth[1], Keith M. Dawson[1], Vladimir Kirkin[1], Adrian F. Ochsenbein[2], Sebastian Grimm[1], Nina Reschke[1], Carsten Riether[2], Daniel Steiner[1], Nicolas Leupin[1*], Anne Goubier[1*]

Affiliations

[1]Molecular Partners AG, Wagistrasse 14, 8952 Schlieren, Switzerland
[2]Department of Medical Oncology, Inselspital, Bern University Hospital, University of Bern, Freiburgerstrasse, 3010 Bern, Switzerland
[*]Equal contribution

Corresponding author

Dr. Anne Goubier
Molecular Partners AG
Wagistrasse 14
CH-8952 Schlieren, Switzerland
Email: anne.goubier@molecularpartners.com
Phone +41 44 755 77 00

Disclosure of Potential Conflicts of Interest

M. Bianchi: reports personal fees from Molecular Partners AG and ownership of Molecular Partners AG stocks during the conduct of the study, and has a patent for US11,834,504 issued to Molecular Partners AG and a patent for WO2022/190016 pending. **C. Reichen:** reports personal fees from Molecular Partners AG and ownership of Molecular Partners AG stocks during the conduct of the study, and has a patent for US11,834,504 issued to Molecular Partners AG and a patent for WO2022/190016 pending. **A. Croset:** reports personal fees from Molecular Partners AG and ownership of Molecular Partners AG stocks during the conduct of the study. **S. Fischer:** reports personal fees from Molecular Partners AG and ownership of Molecular Partners AG stocks during the conduct of the study. **A. Eggenschwiler:** reports personal fees from Molecular Partners AG and ownership of Molecular Partners AG stocks during the conduct of the study. **Y. Grübler:** reports personal fees from Molecular Partners AG and ownership of Molecular Partners AG stocks during the conduct of the study. **R. Marpakwar:** reports personal fees from Molecular Partners AG and ownership of Molecular Partners AG stocks during the conduct of the study. **T. Looser:** reports personal fees from Molecular Partners AG and ownership of Molecular Partners AG stocks during the conduct of the study. **P. Spitzli:** reports personal fees from Molecular Partners AG and ownership of Molecular Partners AG stocks during the conduct of the study. **C. Herzog:** reports personal fees from Molecular Partners AG and ownership of Molecular Partners AG stocks during the conduct of the study. **D. Villemagne:** reports personal fees from Molecular Partners AG and ownership of Molecular Partners AG stocks during the conduct of the study. **D. Schiegg:** reports personal fees from Molecular Partners AG and ownership of Molecular Partners AG stocks during the conduct of the study. **L. Abduli:** reports personal fees from Molecular Partners AG and ownership of Molecular Partners AG stocks during the conduct of the study. **C. Iss:** reports personal fees from Molecular Partners AG and ownership of Molecular Partners AG stocks during the conduct of the study. **A. Neculcea:** reports personal fees from Molecular Partners AG and ownership of Molecular Partners AG stocks during the conduct of the study. **M. Franchini:** reports personal fees from Molecular Partners AG and ownership of Molecular Partners AG stocks during the conduct of the study. **T. Lekishvili:** reports personal fees from Molecular Partners AG and ownership of Molecular Partners AG stocks during the conduct of the study. **S. Ragusa:** reports personal fees from Molecular Partners AG and ownership of Molecular Partners AG stocks during the conduct of the study. **C. Zitt:** reports personal fees from Molecular Partners AG and ownership of Molecular Partners AG stocks during the conduct of the study. **Y. Kaufmann:** reports personal fees from Molecular Partners AG and ownership of Molecular Partners AG stocks during the conduct of the study. **A. Auge:** reports personal fees from Molecular Partners AG and ownership of Molecular Partners AG stocks during the conduct of the study. **M. Hänggi:** reports personal fees from Molecular Partners AG and ownership of Molecular Partners AG stocks during the conduct of the study. **W. Ali:** reports personal fees from Molecular Partners AG and ownership of Molecular Partners AG stocks during the conduct of the study. **T. M. Frasconi:** reports personal fees from Molecular Partners AG and ownership of Molecular Partners AG stocks during the conduct of the study. **S. Wullschleger:** reports personal fees from Molecular Partners AG and ownership of Molecular Partners AG stocks during the conduct of the study. **I. Schlegel:** reports personal fees from Molecular Partners AG and ownership of Molecular Partners AG stocks during the conduct of the study. **M. Matzner:** reports personal fees from Molecular Partners AG and ownership of Molecular Partners AG stocks during the conduct of the study. **U. Luethi:** declares no potential conflicts of interest. **B. Schlereth:** reports personal fees from Molecular Partners AG and ownership of

Molecular Partners AG stocks during the conduct of the study, and has a patent for US11,834,504 issued to Molecular Partners AG and a patent for WO2022/190016 pending. **K. M. Dawson:** reports personal fees from Molecular Partners AG and ownership of Molecular Partners AG stocks during the conduct of the study. **V. Kirkin:** reports personal fees from Molecular Partners AG and ownership of Molecular Partners AG stocks during the conduct of the study. **A. F. Ochsenbein:** reports consultancy fees from Molecular Partners AG during the conduct of the study. **S. Grimm:** reports personal fees from Molecular Partners AG and ownership of Molecular Partners AG stocks during the conduct of the study, and has a patent for US11,834,504 issued to Molecular Partners AG and a patent for WO2022/190016 pending. **N. Reschke:** reports personal fees from Molecular Partners AG and ownership of Molecular Partners AG stocks during the conduct of the study, and has a patent for US11,834,504 issued to Molecular Partners AG and a patent for WO2022/190016 pending. **C. Riether:** reports consultancy fees from Molecular Partners AG during the conduct of the study. **D. Steiner:** reports personal fees from Molecular Partners AG and ownership of Molecular Partners AG stocks during the conduct of the study. **N. Leupin:** reports personal fees from Molecular Partners AG and ownership of Molecular Partners AG stocks during the conduct of the study. **A. Goubier:** reports personal fees from Molecular Partners AG and ownership of Molecular Partners AG stocks during the conduct of the study.

Running title

MP0533, a multispecific LSC-targeting CD3-engaging DARPin

Keywords

- Acute myeloid leukemia
- Leukemic stem cells and blasts
- DARPin
- T-cell engager
- CD33xCD123xCD70

Synopsis

In preclinical studies on the T-cell engager MP0533, the authors show that targeting multiple tumor-associated antigens may lead to better selectivity and efficacy in eliminating leukemic stem cells and blasts, representing a promising therapeutic strategy for AML.

Financial support

All studies were financed by Molecular Partners AG, Schlieren, Switzerland

Abstract

The prognosis of patients with acute myeloid leukemia (AML) is limited, especially for elderly or unfit patients not eligible for hematopoietic stem cell (HSC) transplantation. The disease is driven by leukemic stem cells (LSCs), which are characterized by clonal heterogeneity and resistance to conventional therapy. These cells are therefore believed to be a major cause of progression and relapse. We designed MP0533, a multispecific CD3-engaging DARPin (designed ankyrin repeat protein) that can simultaneously bind to three antigens on AML cells (CD33, CD123, and CD70), aiming to enable avidity-driven T cell–mediated killing of AML cells co-expressing at least two of the antigens. *In vitro,* MP0533 induced selective T cell–mediated killing of AML cell lines, as well as patient-derived AML blasts and LSCs, expressing two or more target antigens, while sparing healthy HSCs, blood, and endothelial cells. The higher selectivity also resulted in markedly lower levels of cytokine release in normal human blood compared to single antigen–targeting T-cell engagers. In xenograft AML mouse models, MP0533 induced tumor-localized T-cell activation and cytokine release, leading to complete eradication of the tumors while having no systemic adverse effects. These studies show that the multispecific-targeting strategy used with MP0533 holds promise for improved selectivity towards LSCs and efficacy against clonal heterogeneity, potentially bringing a new therapeutic option to this group of patients with high unmet need. MP0533 is currently being evaluated in a dose-escalation phase 1 study in patients with relapsed or refractory AML (NCT05673057).

Introduction

Treatment options for patients with acute myeloid leukemia (AML) have increased with the recent introduction of several new drugs targeting abnormal karyotypes, such as FMS-like tyrosine kinase 3 (FLT3) (1) and isocitrate dehydrogenase 1 or 2 (IDH1/2) (2) inhibitors, or targeted effector molecules like B-cell lymphoma 2 (BCL2) inhibitors (3,4) and hypomethylating agents (HMA) (5). Despite these advances, the prognosis of AML patients is still dismal, with a 5-year overall survival (OS) rate of 40-50% for patients younger than 60 years and less than 5% for elderly patients (≥70 years) who in general are not eligible for a stem cell transplant (6). All of this highlights the need for novel therapeutic strategies (7-9). A major factor in treatment failure is the poor ability of current therapies to kill leukemic stem cells (LSCs) whilst sparing healthy hematopoietic stem cells (HSCs), emphasizing the need to develop agents with high selectivity for killing LSCs (10,11). In contrast to differentiated leukemia cells, LSCs are less sensitive to tyrosine kinase inhibitors and drugs inducing hypomethylation (12,13). Furthermore, LSCs have been shown to be resistant to chemotherapy and show a vast capacity for long-term self-renewal (7,14). Targeted immunotherapy in AML has proven to be difficult due to both the lack of AML-specific target antigens and clonal heterogeneity of tumors, within and between patients (15). Investigation of T-cell engager (TCE) therapies targeting single AML antigens has been hampered by toxicities resulting from on-target binding to healthy HSCs and myeloid cells, as well as to relapse from the outgrowth of leukemic clones not expressing the targeted antigen. To overcome this, it has been proposed that combinatorial targeting of multiple antigens on AML blasts and LSCs might enhance therapeutic efficacy (16,17), ideally without increasing toxicity.

Here we report nonclinical results of an off-the-shelf approach to combinatorial targeting of AML by a multispecific T-cell engaging designed ankyrin repeat protein (DARPin). MP0533 was designed to bind CD3 on T cells while simultaneously binding three AML tumor-associated antigens (TAAs) that have been targeted individually by investigational immunotherapy agents: CD33 (18-21), CD123 (22-24), and CD70 (25). These targets are expressed and co-expressed on AML blasts and LSCs (26,27). While CD70 is not detectable in normal tissue and on HSCs or other hematopoietic cells during homeostasis (28,29), CD33 and CD123, which are low or absent on HSCs (26,27), are present on healthy hematopoietic cells, potentially leading to off-tumor toxicities of single-targeting agents. The optimal binding affinity of MP0533 to each TAA is intended to enable an avidity-like selectivity and efficacy window to preferentially kill AML cells co-expressing at least two of these TAAs while sparing single-expressing healthy cells. Our findings show that MP0533 was indeed able to induce selective killing of AML blasts and stem/progenitor cells (defined throughout the text as LSCs). In line with this, MP0533 demonstrated markedly reduced cytokine release both in *ex vivo* studies and in mouse xenograft models, while maintaining potent antitumor activity *in vivo*.

Materials and Methods

MP0533 generation

Selection of DARPin domains against CD33, CD123, CD33, and CD3. DARPin libraries (30) (N2C) were used in ribosome display selections (31,32) against recombinant protein targets of CD33, CD123, CD70, and CD3. Specifically, the following targets were used: a) CD33 and CD123: extracellular domain of human CD33 or CD123 containing a C-terminal Fc-

and an Avi-tag which were biotinylated using the enzyme BirA (produced in-house); b) CD70: extracellular domains of human CD70 (ACROBiosystems) containing a C-terminal Fc-tag which was chemically biotinylated using 5-fold excess of biotin; and c) CD3: single-chain heterodimeric extracellular domain of human CD3epsilon (CD3e) and CD3gamma (CD3g) linked by a 26 amino acid linker (scCD3eg) and a C-terminal Avi-tag for site-directed biotinylation. scCD3eg was expressed as previously described (33) in *Escherichia coli (E. coli)*, followed by refolding from inclusion bodies and purified by preparative size exclusion chromatography (SEC). The material was up-concentrated in 10 mM Tris-HCl, 50 mM NaCl, pH 8.0 to 3.4 mg/ml and *in vitro* biotinylated using recombinant BirA. To isolate functional target material, the material was re-purified using an OKT3-loaded column (HiTrap NHS-activated HP column, Cytiva). The final material was monomeric on size exclusion and stored at the final concentration of 0.39 mg/ml in 10 mM Tris, 100 mM NaCl, pH 8.0, 10% glycerol.

For each target, four selection rounds were performed with the selection stringency continuously increased by decreasing target concentration and increasing washing incubation time over rounds. For CD3 selection rounds 2-4, mRNA was recovered by competitive elution using an excess of CD3 binding antibody OKT3 (produced in CHO expression system with a human IgG2 heavy and kappa light chain).

To enrich for DARPins with high affinity binding for CD33, CD123, and CD70, the output from the fourth round of standard ribosome display selection (above) was subjected to an off-rate selection round with increased selection stringency (32). A final standard selection round was performed after the off-rate selection round to amplify and recover the off-rate selected DARPins.

Functional screening of the CD3-binding DARPin. Screening of the CD3-binding DARPin was conducted in bivalent format by cloning the domains into derivatives of the pQE30 (Qiagen) expression vector containing a Jun leucine-zipper construct with His-tag, which allowed testing for functionality by cross-linking of T-cell receptors and activation of T cells. In short: single colonies were picked into a 96-well plate (each clone in a single well) containing 160 µl growth medium (TB medium containing 1% glucose and 50 µg/ml ampicillin [Carl Roth]) and incubated overnight at 37°C, shaking at 800 rpm. 150 µl of fresh TB medium containing 50 µg/ml ampicillin was inoculated with 8.5 µl of the overnight culture in a fresh 96-well plate. After incubation for 120 min at 37°C and shaking at 850 rpm, expression was induced with Isopropyl β-D-1-thiogalactopyranoside (IPTG, dioxan-free, Apollo Scientific) (0.5 mM final concentration) and continued for 4 h. Cells were harvested, and the pellets frozen at -20°C overnight before resuspension in 8.5 µl B-PERII (ThermoFisher Scientific) and incubation for 1 h at room temperature (RT) with shaking at 600 rpm. Then, 160 µl PBS (Gibco) was added and cell debris was removed by centrifugation (3,220 g for 15 min) and stored at -20°C for further usage. For the CD3 functional screen, a T-cell activation screen was performed using BK112 $CD8^+$ monoclonal T cells (34,35) (kindly provided by Dr. Victor Levitsky). The extract of each lysed clone was applied as a 1:20 dilution (final concentration) in PBSB (PBS pH 7.4 supplemented with 12% [w/v] fetal bovine serum [FBS, Biowest]) to an anti-penta-His-antibody (Qiagen) coated 96-well plate and incubated at 4°C overnight. Plates were washed five times with PBS before 100 µl with 100,000 BK112 T cells were added per well, cultured in T-cell assay medium (RPMI-1640 [Gibco] containing 10% FBS, 1% L-glutamine [Gibco], 1% Penicillin/Streptomycin [Gibco], and 200 IU IL-2 [Peprotech]). 0.1 µg/100 µl of Golgi Stop (BD Biosciences) were added and plates were centrifuged at 200 g for 3 min at RT before incubation for 4-5 h at 37°C in a CO_2 incubator. Cells were centrifuged at 350 g for 5 min at 4°C and the supernatant decanted. Cells were stained for surface CD8 expression before preserving the cells using Cytofix (BD Biosciences),

incubated overnight at 4°C. Cells were washed with PBS + 2% FBS and stained for intracellular IFNγ by adding 50 µl of anti-IFNγ-APC (BioLegend, clone B27 in Cytoperm buffer (BD Biosciences) and incubating for 30 min at 4°C. Cells were washed again in PBS and analyzed using a Cytometer FACS Canto II and FlowJo analysis software (version 10) (BD Biosciences).

Identified functional DARPin hits were subcloned into derivatives of the pQE30 (Qiagen) expression vector containing an N-terminal His-tag, a Her-2 binding DARPin (G3 derivative (36)) and CD3 binding DARPin. Constructs were expressed in *E. coli* and purified using their His-tag according to standard protocols (37). Binding to recombinant protein was tested using a homogeneous time-resolved fluorescence (HTRF) assay using 48 nM human biotinylated scCD3eg. In brief, HTRF was performed in a 384-well plate using a DARPin protein dilution range of 5-640 nM in PBSTC (PBS, 0.1% Tween-20 [Sigma-Aldrich], 0.1% [w/v] Casein [Sigma-Aldrich], pH 7.4) and 48 nM of biotinylated scCD3eg target, and was detected with anti-6His-d2 HTRF (Cisbio, 1:100) and anti-strep-Tb (Cisbio, 1:100) after 120 min incubation at RT. The plates were measured with a Tecan M1000 using standard HTRF settings.

Competitive binding was observed in the presence of a 20-fold excess of CD3 binding antibody OKT3 (BioLegend). Dose-dependent *in vitro* T-cell activation was confirmed (EC50 = 0.4 nM) using a BK112 T-cell activation assay (BK112 $CD8^+$ monoclonal T cells which were pre-activated with CD3/CD28 Dynabeads [ThermoFisher Scientific]), in the presence of ($HER2^+$) SKOV3 cells.

To improve the affinity of the parental low affinity binding CD3 DARPin, three additional rounds of affinity maturation were conducted by using error-prone PCR and DNA shuffling combined with rational design, as previously described (32).

Screening of CD33, CD123, and CD70 DARPin binding domains. Initial screening of DARPin molecules was performed by HTRF binding assays using crude extracts of DARPin-expressing *E. coli* cells using standard protocols with the following modifications: a) CD70 DARPins were screened in standard monovalent format, and b) CD33 and CD123 DARPins were screened in a bispecific format, by cloning the different domains into derivatives of the pQE30 (Qiagen) expression vector, which contains a C-terminal CD3-specific DARPin followed by a Flag-tag. Screening for binding was performed in crude extract by HTRF. In short: HTRF was performed by using crude extract dilutions in PBSTB (PBS, 0.1% Tween-20, 0.2% [w/v] bovine serum albumin [BSA, from Sigma-Aldrich], pH 7.4) (final dilution was 1:2000 for CD70, and 1:1000 for CD123 and CD33) and biotinylated target (2 nM for CD70, 4 nM for CD123, 6 nM for CD33) and detected as described above.

To further optimize binding of the initially identified DARPins to the different TAAs, binders with very high affinity were generated by affinity maturation. Thereby, initially identified binding DARPins (the "parental" binding DARPins) with desirable activity and developability profiles were selected as starting points for affinity maturation for each TAA. First, the affinity maturation procedure entailed saturation mutagenesis of each randomized position of the ankyrin repeat domain used. Sequences generated by the affinity maturation procedure were then screened for lower off rates by competitive HTRF. In short: crude extracts of ankyrin repeat proteins, containing an N-terminal His-flag-tag were incubated with the biotinylated target before the addition of at least a 1000-fold excess of non-flag-tagged parental DARPin (1,000-fold for CD70, and 2,500-fold for CD123 and CD33) and measurement of HTRF signal over time. Beneficial mutations, identified based on higher HTRF signals compared to parental clone, were combined in the binding proteins by rational protein engineering.

Engineered DARPin hits showed improved *in vitro* T-cell activation EC50 compared to parental clones by 6-fold for CD70, 52-fold for CD123, and 66-fold for CD33. Affinity matured DARPins hits were subcloned into derivatives of the pQE30 (Qiagen) expression vector, containing an N-terminal His-tag, followed by the TAA binding DARPin variant and a C-terminal CD3 binding DARPin. Constructs were expressed in *E. coli* cells and purified using their His-tag according to standard protocols.

Generation of multi-specific DARPin molecule MP0533. For the generation of the multi-specific T-cell engaging DARPin molecule MP0533, targeting simultaneously three different TAAs, multiple optimization steps were applied. In a first step, combinations of CD123- and CD33-targeting T-cell engagers (TCEs) were screened for an avidity-driven selectivity window measured by T-cell activation and tumor cell killing using MOLM-13 N1 (CRISPR control) and MOLM-13 knock out (KO) cells (KO for CD33, CD123, CD70, and combinations thereof, generated as described below). In a second step, a third TAA-binding DARPin against CD70 was introduced. Again, CD70 binders were used to generate a selectivity window when at least two TAA are expressed on the target cells. Additionally, two N-terminal human serum albumin (HSA)-binding DARPin were introduced for half-life extension (38). Third, in order to achieve high potency on primary samples from patients (expressing lower TAA levels compared to MOLM-13 cells or other AML cell lines), several rational design approaches were conducted to improve the molecule, including a) the usage of affinity matured variants of initial TAA-binding or CD3-binding DARPins, and b) format optimization (optimal orientation of TAA-binding domains). For format optimization, combinations of 4-6-domain constructs, all containing 1-2 N-terminal anti-HSA domains followed by 2-3 domains that specifically bind to the TAAs on AML cells and a C-terminal CD3-binding domain were generated by using a Gibson assembly or standard cloning approach with suitable restriction enzymes. All individual DARPins were linked with standard proline-threonine-rich polypeptide linkers (31). The constructs were all cloned into derivatives of pQE30 (Qiagen) expression vector. Correctly assembled constructs were then transformed into *E. coli* BL21, expressed and purified using their His-tag according to standard protocols.

Once the optimal CD33, CD123, and CD70-specific DARPins were identified, multispecific DARPins with permutations of the TAA-binding domains were generated and the constructs screened again for functional activity. The final order of the TAA-specific DARPins in MP0533 (CD33–CD123–CD70) resulted in the best therapeutic window towards MOLM-13 cells expressing at least two TAAs vs. only one TAA (Supplementary Fig. S1A), reduced killing of CD123-expressing HUVEC (Supplementary Fig. S1B), reduced depletion of healthy white blood cells and platelets (Supplementary Fig. S1C), and reduced induction of cytokine release in healthy whole blood (Supplementary Fig. S1D and E) compared to other tested formats (CD70–CD123–CD33 and CD70–CD33–CD123).

Negative-control DARPins lacking either TAA- or CD3-binding domains were also generated, using non-binding DARPins instead. Control DARPins used in these studies, named NB-CD3 and TAA-NB, are both composed of six domains: HSAxHSAxNBxNBxNBxCD3 and HSAxHSAxCD33xCD123XCD70XNB, respectively (where NB represent the same non-specific DARPin).

Surface plasmon resonance (SPR) affinity determination

In addition to binding to human CD33, CD123, CD70, CD3, and HSA (hCD33, hCD123, hCD70, hCD3, HSA) (Table 1 and Supplementary Fig. S2A), cross-reactive binding to

cynomolgus target material was observed for CD123 and CD70 (cCD123, cD70) with respective affinities of 12 nM and 0.2 nM (208- and 3-fold increase compared to human, respectively), while no binding to cynomolgus CD3 and CD33 was observed. The HSA-binding DARPin in MP0533 has also been used in other clinical-stage DARPins (eg MP0317 or MP0310) and is cross-reactive to both cynomolgus and mouse serum albumin. No cross-reactivity to target mouse proteins other than serum albumin was observed. For all targets, affinities were measured by SPR as indicated below.

SPR measurements against hCD33, hCD70, hCD3, HSA, and cCD70 were performed using a ProteOn XPR36 instrument (Bio-Rad), and against hCD123 and cCD123 with a Sierra SPR-32 Pro instrument (Bruker). The running buffer was PBS pH 7.4 containing 0.005% Tween 20 (PBST) for all measurements.

For hCD33, hCD3, and HSA, a Xantec HC200M sensor chip was initialized and conditioned according to the manufacturer's protocol. The sensor chip was activated with EDAC/NHS (1:1, 300 sec, 30 µl/min), MP0533 was immobilized to ~1400 Rus (10 µg/ml in 10 mM NaOAc pH 4.0, 30 µl/min, 50 sec), and the surface was deactivated with 1 M ethanolamine for 300 sec, 30 µl/min. The analyte hCD33 was injected at 66.7-0.82 nM, 240 sec on-rate and 500 sec off-rate were recorded (100 µl/min). A pause of 10 min was introduced between the triplicates measured. The data was double-referenced (interspot + L6 buffer reference) and globally fitted to a 1:1 Langmuir model. The experiment for measuring affinity binding of MP0533 to hCD3 (using scCD3eg) was conducted in the same way as described for hCD33 with the following modification: MP0533 was immobilized to ~1600 Rus (18.2 µg/ml in 10 mM NaOAc pH 4.5, 30 µl/min, 1050 sec), and the analyte hCD3 was injected at 450-5.6 nM (in 3-fold dilutions). The experiment for measuring affinity binding of MP0533 to HSA was conducted in the same way as described for hCD33 with the following modification: the analyte concentration of HSA was 450 nM-5.6 nM (in 3-fold dilutions).

For hCD70 and cCD70, a Xantec PAGD200L Protein A/G sensor chip was initialized and conditioned according to the manufacturer's protocol. hCD70 (hCD70-Fc-trimer) was captured ~200 Rus (10 µg/ml, 10 µl/min, 33 sec). The analyte MP0533 was injected in a three-fold dilution series of 600-7.4 nM; 240 sec on-rate and 2700 sec off-rate are recorded (100 µl/min). The surface was regenerated with a 18 sec pulse of 10 mM glycine, pH 2.0, 100 µl/min before fresh ligand was captured. The data was double-referenced (interspot + L6 buffer reference) and globally fitted to a 1:1 Langmuir model. Due to drift, the highest concentration (600 nM) was omitted from the analysis. The experiment for measuring affinity binding of MP0533 to cCD70 was conducted in the same way as described for hCD70 with the following modification: cCD70 (5x BioCD70 cyno (CD27 Ligand)) was captured to ~320 Rus (1.25 µg/ml, 30 µl/min, 50 sec) before running dilution series of MP0533 (150 nM-1.9 nM), recording association for 240 sec (25 µl/min) and dissociation for 7200 sec (25 µl/min). No regeneration was needed because measurement for cCD70 was conducted only once.

For hCD123 and cCD123, a Bruker IgG Capture sensor chip was initialized and conditioned according to the manufacturer's protocol. hCD123 was captured to ~150 Rus (0.95 µg/ml, 10 µl/min, 50 sec). A dilution series from 200 nM – 91 pM of MP0533 (3-fold dilutions) was prepared and injected sequentially in triplicates. Association was recorded for 240 sec (25 µl/min), dissociation was measured for 1500 sec (25 µl/min). The surface was regenerated with a 20 sec pulse of 10 mM glycine, pH 2.0, 25 µl/min before fresh ligand was captured. After each capture, a PBST blank injection was performed (240 sec injection, 1500 sec off-rate, 25 µl/min). The sensorgrams were double referenced (surface and buffer). The

triplicates measured were globally fitted according to a 1:1 Langmuir model. The experiment for measuring affinity binding of MP0533 to cCD123 was conducted in the same way as has been described for cCD123 with the following modification: cCD123 was captured to ~150 Rus (10 µg/ml, 10 µl/min, 50 sec) before running serial dilutions of MP0533, recording association for 240 sec (25 µl/min) and dissociation for 600 sec (25 µl/ min).

Simultaneous binding of MP0533 to all its targets

SPR measurements were performed on a Sierra SPR-32 instrument (Bruker). PBS pH 7.4 containing 0.005% Tween 20 was used as running buffer. 2600 Rus of 300 nM HSA was immobilized on an HCA sensor chip. To the HSA immobilized chip successively 1 µM MP0533 (association 60 sec, dissociation 0 sec), 200 nM hCD70 (association 40 sec, dissociation 0 sec), and 500 nM hCD123 (association 120 sec, dissociation 0 sec) were applied as independent analyte injection steps. Immediately after, a dual injection step was performed injecting 150 nM hCD33 (association 150 sec, dissociation 0 sec) followed by 1.35 µM hCD3 (association 150 sec, dissociation 180 sec). The setup allows binding of hCD70, hCD123, hCD33, and hCD3 only if MP0533 is already bound to HSA. A requirement for this set-up was that MP0533 binds HSA with high avidity and hCD70/hCD123 with high affinity to prevent rapid signal loss before applying the last targets. To overcome the faster dissociation rates of hCD33 and hCD3, a dual injection was used for these targets to shorten the time between hCD33 injection stop and hCD3 injection start. Furthermore, single injections control runs have been conducted by injecting none (PBST) or only one of the targets (Analyte 2-5) as described in injection scheme in Supplementary Table S1. The signals were referenced to an empty control spot on the same channel. All steps were performed at a flow rate of 10 µl/min, except for the dual injection at 20 µl/min (20 µl/min is the lowest flow rate possible using the dual-injection mode).

Generation of non-DARPin reference molecules

All non-DARPin comparator molecules used in this study were produced in CHO cells by Evitria (Schlieren, Switzerland).

The CD33-CD3 Bispecific T-cell Engager (BiTE) molecule binding to human CD33 and CD3 was produced as a single-chain antibody using the sequence of patent WO2017129585 (sequence 100 – referred to as AMG330 (39)) containing in addition a C-terminal His-tag for purification.

The CD33-CD3 bivalent molecule, consisting of two binding domains for CD33 and CD3 each, was produced as a TandAbs by using the sequence of Vixtimotamab described in INN Recommended List 86 with the addition of a C-terminal His-tag (WHO Drug Information, vol. 35, no. 3, 2021 – referred to as T564 (40) or AMV564 (18)).

The CD123-CD3 Dual-Affinity Re-Targeting (DART) molecule binding to human CD123 and CD3 was produced using the sequence of patent US9822181B2 (sequences 1 and 3 – referred to as MGD006 (41)). A C-terminal Flag- and His-tag was added to sequence 1 and 3, respectively (42).

The half-life extended (HLE)-CD123-CD3 DART molecule binding to human CD123 and CD3 was produced as DART molecule containing an Fc for half-life extension using the sequence of patents US_2021_0155694_A1 (sequence 179) and WO2021257334 (sequences 28 and 30, putative MGD024 (43)).

The CD123-CD3 ADAPTIR molecule, consisting of two binding domains to CD123 and CD3 each, and an Fc for half-life extension, was produced using the sequence from patent WO_2021_146328 (sequence 337 – referred to as APVO436 (23)).

Mice

NXG mice (NOD-*Prkdc*^{scid}-*IL2rg*^{Tm1}/Rj) were obtained from Janvier and NSG mice (NOD.Cg-Prkdcscid Il2rgtm1Wjl/SzJ) from Charles River Laboratories. All mice were housed in accredited animal facilities and maintained in specific pathogen-free conditions. Female 8-to-12-weeks-old mice were used in all experiments. Experiments performed with NXG mice at Molecular Partners AG (Switzerland) and NSG mice at the University of Bern (Switzerland) were done according to the Swiss Animal Protection Law with authorization from the cantonal and federal veterinary authorities (study protocols PD1091, PD1094, PD1095, and PD1101 approved under license ZH2013/16, CH23590).

Cell lines

MOLM-13 (ACC-554, RRID CVCL_2119, received in 2015), OCI-AML-5 (ACC-247, RRID CVCL_1620, received in 2015), and THP-1 (ACC-016, RRID CVCL_0006, received in 2016),were purchased from DMSZ (Deutsche Sammlung von Mikroorganismen und Zellkulturen); MV4-11 (CRL-9591, RRID CVCL_0064, received in 2015), HL-60 (CCL-240, RRID CVCL_0002, received in 2015), KG1a (CCL-246.1, RRID CVCL_1824, received in 2019), U937 (CRL-1593.2, RRID CVCL_0007, received in 2010), RPMI8226 (CRM-CCL-155, RRID CVCL_0014, received in 2013), and SKOV3 (HTB-77, RRID CVCL_0532, received in 2016) from ATCC (American Type Culture Collection); MOLM-13 LUC (received in 2021) from Creative Biolabs (IOC-02P004); HUVEC (received in 2015) from Lonza (C2519A). All suspension cell lines were maintained at a density of 0.5×10^6 - 2×10^6 cells/ml in RPMI 1640 (Gibco) supplemented with 10% FBS (Biowest) at 37°C, 5% CO_2. SKOV3 cells were grown in McCoy's 5A (Gibco) + 10% FBS. HUVEC were cultured in EGM-2 (Lonza) supplemented with 5% FBS, 20 µM HSA (CSL Behring), and Endothelial Cell Growth Medium Supplement Mix (PromoCell). Cells were passaged every 2 to 4 days and number of passages was limited to 20 (or 5 for HUVEC). All cell lines were tested for mycoplasma (MycoAlert mycoplasma detection kit; Lonza) and have not been reauthenticated within the past year.

Patient samples: ethical statement

Whole blood from healthy donors was obtained from Swiss Red Cross (SRK) blood donation centers or Immuneed (Sweden), and buffy coats from SRK centers. Bone marrow of healthy donors or AML patients was collected by the University Hospital of Bern (Switzerland), and by hospitals collaborating with Vivia Biotech (Spain). All human samples were analyzed with the approval of local ethical committees, in accordance with local regulations and the principles of the Declaration of Helsinki. Written informed consent was obtained from each participant.

Isolation of mononuclear and pan T-cells

Buffy coats or bone marrow samples from healthy donors or AML patients were diluted with PBS and PBMCs or BMMCs isolated by density-gradient centrifugation using LeucoSep tubes (Greiner) according to the vendor's manual. Pan T cells were purified from PBMCs using a negative selection human pan T cell isolation Kit (Miltenyi) according to the manufacturer's recommendations (Greiner), and then used fresh or after freezing at -180°C in CryoStor CS10 medium (STEMCELL Technologies). If needed, total pan T cells were stained with Cell Trace Violet (CTV; ThermoFisher Scientific) at a ratio of 1 µl dye per $30x10^6$ T cells/ml in PBS. After 20 min incubation at RT and protection from light, cells were washed with complete culture medium to quench and remove free remaining dye.

TAA expression on healthy whole blood cells

A total of 200 µl whole blood were added per well to a round-bottom 96 well plate and the erythrocytes lysed with High-Yield Lyse Fixative-Free Lysing Solution (Life Technologies) according to the manufacturer's instructions. After 2 wash steps with 200 µl PBS + 2% FBS (FACS buffer), 50 µL of human Fc blocking reagent (BD Biosciences), diluted in Brilliant Stain Buffer (BD), was added for 15 min at 4°C. Antibodies and viability reagent were prepared in FACS buffer. The lowest saturating concentration was used for each antibody to reduce the spreading error. After blocking, 50 µl of the staining antibody mixture was added on top of the blocking solution. To aid gating and calculation of median fluorescence intensities (MFIs), fluorescence minus one (FMO) stained cells were prepared for CD33, CD123, and CD70. The staining mixture was incubated for 40 min at 4°C. Cells were then washed twice in FACS buffer + 2 mM EDTA, fixed for 30 min in 1x Cell-Fix (BD Biosciences) at 4°C, washed twice again, and resuspended in PBS + 2 mM EDTA for acquisition. The panel of antibodies used is summarized in Supplementary Table S2 and the markers used for the identification of different cell populations are summarized in Supplementary Table S3. Representative flow cytometry plots and gating are shown in Supplementary Fig. S3A.

Acquisition was performed using an Aurora 4L 16V-14B-10YG-8R Full Spectral Flow Cytometer (SFC) (Cytek) within 24 hours of staining. The machine was calibrated using fluorescent standard setup beads to provide reproducible day-to-day performance and consistency over time. Settings used for acquisition on SFC Aurora were: FSC 48; SSC 160; SSC-B 164; Thr 200k. To provide data for channel unmixing, single stained controls were performed using healthy donor whole blood. Ten seconds of delay was applied before commencing acquisition, acquisition speed was limited to medium, 4 sec mixing was applied before acquisition and the plate reader was cooled to 5°C prior to acquisition. Unmixed files were exported and analyzed using FlowJo analysis software (version 10) and MFIs exported to Excel (Microsoft) for further analysis. Visualizations were performed using Graph Pad Prism (version 9).

Quantification of data for CD33, CD123, and CD70 was achieved using the Quantum Simply Cellular (QSC) system as per the manufacturer's instructions (Bangs Laboratories). QSC Anti-mouse IgG consists of one blank and 4 calibration beads, bearing a range of receptors from ~3k to 300k. Beads were stained using a saturating concentration of antibody using the same method as for cells and acquired without fixation. The MFI values were applied to a provided standard curve for the calculation of antibody binding capacity (ABC) of the population and antigen of interest. The regression coefficient and detection threshold are also calculated.

Generation of MOLM-13 KO cell lines

MOLM-13 cells were genetically modified using TAA-specific CRISPR guide RNAs (all from IDT) (CD33: GACAACCAGGAGAAGATCGG; CD123: GACCAACTACACCGTCCGAG; CD70: CTCACCCCAAGTGACTCGAG and AGCGCTGGATGCACACCACG) to KO selected TAAs, or by a non-targeting guide RNA (Alt-R CRISPR-Cas9 Negative Control crRNA#1, IDT #1072544) as CRISPR control to generate the N1 cell line. Generation of all KO cell lines was performed sequentially. Successfully modified cells were single-cell sorted by flow cytometry, and the resulting clones expanded and validated by both binding and functional assays using CD33, CD123, or CD70 single-targeting antibodies (clones WM53, 6H6, and 113-16, respectively) or TCEs (CD33-CD3 BiTE, CD123-CD3 DART, CD70-CD3 DARPin, respectively).

TAA expression on MOLM-13 KO clones

All cell clones were collected, counted with Luna FL (Logos Biosystems), and seeded at $1x10^5$ cells/well in a round-bottom 96 well plate. Cells were pelleted by centrifugation at 350 g for 5 min at 4°C (used for all centrifugation steps) and then washed once with PBS + 2% FBS (Biowest) (FACS buffer). Antibodies for TAA-detection (anti-human CD33 [WM53] and CD123 [6H6] diluted 1:50, and CD70 [113-16] diluted 1:200; all antibodies from BioLegend) and isotype controls were prepared in FACS buffer. The cell pellets were resuspended in 100 µl/well of antibody or isotype control dilution and incubated for 45 min at 4°C. 150 µl FACS buffer was added after incubation and the cells were again pelleted by centrifugation, followed by another washing step with 200 µl FACS buffer. Cells were then resuspended in 100 µl LIVE/DEAD fixable cell stain (1:3,000, ThermoFisher Scientific) diluted in PBS and incubated for 20 min at 4°C. Finally, the cells were washed again twice with PBS and fixed using BD Cell Fix solution diluted 1:10 in water according to the manufacturer's recommendations. TAA expression was assessed by flow cytometry using FACS Attune Nxt (ThermoFisher Scientific). The instrument compensation was performed with compensation beads according to the manufacturer's recommendations (ArC Amine Beads for LIVE/DEAD dye and UltraComp eBeads for labeled antibodies, both from ThermoFisher Scientific). Raw flow cytometry standard files (fcs) were exported and analyzed using FlowJo software (version 10). Cell gating was applied to identify the cells of interest, single cells, and to discriminate live cells. Overlay histograms of isotype controls and antibody staining were exported from FlowJo. MFI values were exported from FlowJo and plotted using GraphPad Prism software (version 9).

TAA quantification on cell lines

Quantification of TAAs was performed using QIFIKIT (Agilent Dako) according to the manufacturer's instructions. Briefly, cells were centrifuged at 350 g for 5 min at 4°C (same centrifugation step throughout the whole staining procedure) and then washed once with PBS. Total cell numbers were obtained with Luna FL (Logos Biosystems), and then $1x10^5$ cells/well were seeded in a round-bottom 96 well plate in 100 µl PBS. First, 2 µl of human Fc block (BD Biosciences) was added to the wells (2.5 µg/ml final concentration) and incubated for 10 min at RT, then 2 µl of TAA-specific antibody (pre-diluted to 125 µg/ml) was added on top (again to have 2.5 µg/ml final concentration) and incubated for 30 min at 4°C. Cells were then centrifuged and washed with FACS buffer and the supernatant discarded. Cell pellets were resuspended in 100 µl of 1:50 diluted fluorescein isothiocyanate (FITC)-conjugated

anti-mouse secondary antibody (included in QIFIKIT) and incubated 45 min at 4°C in the dark. Finally, the cells were washed again with PBS, fixed using BD Cell Fix solution diluted 1:10 in water according to the manufacturer's recommendations (BD Biosciences), and finally resuspended in PBS for the analysis.

Target expression by antibody binding on cells was then assessed by flow cytometry using a FACS Canto II (BD Biosciences). To establish the proper fluorescence range for the analysis, the configuration of the instrument was performed with the provided setup beads according to the manufacturer's recommendations. Cell gating was applied to exclude debris and identify FITC-positive cells to determine the expression of TAAs on all different cell lines. MFI values were exported from FlowJo (version 10) as raw fcs files and normalized to the values obtained with the isotype control antibody (background correction). The antibody binding capacity for each TAA was interpolated from the generated standard curve obtained with the provided calibration beads and plotted using GraphPad Prism software (version 9).

Binding of MP0533 to cell lines and pan T cells

Cell lines or pan T cells were washed with PBS and then seeded at $1x10^5$ cells/well in a round-bottom 96-well plate. Cells were pelleted by centrifugation at 400 g for 5 min at 4°C (used for all centrifugation steps). DARPin dilutions were prepared at 500 nM in FACS buffer containing 10 µM HSA (note that all subsequent washing and staining steps in FACS buffer contained 10 µM HSA; CSL Behring) and serially diluted 1:5 for a total of 8 dilutions. The cell pellets were resuspended in 50 µl DARPin dilutions per well and incubated for 1 h at 4°C. 150 µl FACS buffer was added after incubation and the cells were again pelleted by centrifugation, followed by another washing step with 200 µl FACS buffer + HSA. Cells were then resuspended in 50 µl rabbit anti-DARPin 1.1.1 (2 µg/ml, unlabeled, produced in house) + LIVE/DEAD fixable cell stain (1:3,000 diluted in PBS, Thermo Fisher Scientific) diluted in FACS buffer + HSA. After 1 h incubation and two washing steps with 200 µl FACS-buffer + HSA, a secondary goat anti-rabbit-AF647 antibody (1:1,000, ThermoFisher Scientific) was added and again incubated for 30 min at 4°C. Finally, the cells were washed again twice with PBS and fixed using BD Cell Fix solution diluted 1:10 in water according to the manufacturer's recommendations. Cell binding was assessed by flow cytometry using a FACS Canto II (BD Biosciences). The instrument compensation was performed with compensation beads according to the manufacturer's recommendations (ArC Amine Beads for LIVE/DEAD dye and UltraComp eBeads for labeled antibodies, both from ThermoFisher Scientific). Raw fcs files were exported and analyzed using FlowJo software (version 10). Cell gating was applied to identify T cells, single cells, and to discriminate live cells using LIVE/DEAD dye. MFI values were exported from FlowJo and plotted using GraphPad Prism software (version 9).

In vitro human $CD8^+$ T-cell activation and tumor cell killing assay

Freshly isolated, Cell Trace Violet (CTV; ThermoFisher Scientific)-stained pan T cells ($1x10^5$ cells/well) were co-incubated with indicated AML cell lines ($2x10^4$ cells/well) at a 5:1 ratio (to reach complete killing, an E:T ratio of up to 5:1 was used for experiments performed within 48 h, while 1:1 was used for experiments lasting 72 h or longer) in RPMI 1640 medium (Gibco) + 10% FBS (Biowest) and 10 µM HSA (to provide saturation of the HSA-binding DARPins; CSL Behring) in 96-well plates together with titrations of MP0533 or comparator molecules. Cultures were incubated for 48 h at 37°C, 5% CO_2. Supernatants for cytokine release determination were collected and stored at -80°C until further analysis (see below).

CD25 upregulation on $CD8^+$ T cells, as well as the percentage of killed tumor cells were assessed by flow cytometry (staining of cells and acquisition described below). Isolated pan T cells were used in all killing assays reported in this study, as no difference in cytotoxicity and relative release of cytokines was observed vs. PBMCs (Supplementary Fig. S4).

Cell staining for flow cytometry acquisition and analyses

Cells were washed with 150 µl PBS, centrifuged at 1,800 rpm for 2 min at 4°C, the supernatant discarded, and the cell pellet resuspended in 50 µl of LIVE/DEAD fixable cell stain (1:3,000 diluted in PBS; ThermoFisher Scientific). After an incubation time of 30 min at 4°C, cells were washed as described above, and the cells resuspended in 50 µl antibody cocktail against human CD8a (RPA-T8) (1:400; BioLegend) and CD25 (BC96) (1:100; BioLegend) diluted in PBS + 2% FBS (Biowest). After 30 min incubation at 4°C and in the dark, cells were washed again with PBS and fixed using BD Biosciences Cell Fix buffer diluted 1:10 in water according to the manufacturer's recommendations.

Instrument (FACS Canto II [BD Biosciences] or Attune NxT [ThermoFisher Scientific]) compensation was performed with beads according to the manufacturer's recommendations (ArC Compensation Beads for LIVE/DEAD dye and UltraComp eBeads for labeled antibodies, both from ThermoFisher Scientific). Raw fcs files were exported and analyzed using FlowJo software (version 10). Cell gating was applied to discriminate live cells using LIVE/DEAD dye, followed by gating on $CD8^+CD25^+$ cells to determine the population of activated T cells. Killing of tumor cells was evaluated by absolute cell counting of living CTV^- cells per fixed volume (90 µl). MFI and percentage values were exported from FlowJo and plotted using GraphPad Prism software (version 9). EC50 values were determined by converting the x values (concentrations) in log scale and fitting a non-linear mode log (agonist) vs. response with a variable slope (three parameters) equation.

Kinetics of T-cell activation

Freshly isolated pan T ($5x10^4$ cells/well) and MOLM-13 cells ($5x10^4$ cells/well) were co-incubated at 1:1 ratio (generally used for experiments lasting 72 h or longer, while up to 5:1 was used for experiments performed within 48 h) in RPMI 1640 medium + 10% FBS and 10 µM HSA (to provide saturation of the HSA-binding DARPins; CSL Behring) in round-bottom 96-well plates together with titrations of MP0533 or comparator molecules in 200 µl final volume. Co-cultures were incubated for various times (24 h, 48 h, 5 days, 8 days) at 37°C and 5% CO_2 and then the cells were analyzed for various markers related to T-cell activation, proliferation, exhaustion, and cytotoxic granules.

At all timepoints analyzed, cells were washed with PBS and incubated with 100 µl Fc-block (1:100, BD Biosciences) for 20 min at RT. After an additional wash step with 100 µl PBS, cells were incubated with FVD eFluor 506 dye (ThermoFisher Scientific) in PBS (1:600) for another 20 min at 4°C in the dark. In a next step, cells were washed with 100 µl FACS buffer and stained for surface markers by using directly labeled antibodies against human CD4 (OKT4, 1:200), CD8a (RPA-T8, 1:100), CD25 (BC96, 1:200), CD69 (FN50, 1:100), PD-1 (EH12.2H7, 1:100), LAG-3 (7H2C65, 1:200), and TIM-3 (F38-2E2, 1:200) (all from BioLegend) in 100 µl FACS buffer for 30 min at 4°C in the dark. Two washes were then performed, first with 100 µl and then 200 µl FACS buffer, before continuing with cell permeabilization. Intracellular staining was performed according to Invitrogen's protocol from the FoxP3 transcription factor buffer kit (Invitrogen): cells were washed and permeabilized with

permeabilization/fixation buffer for 20 min at RT, followed by 20 min incubation with antibodies specific for intracellular markers (Ki-67, 1:200 [BD Biosciences] and Granzyme B, 1:100 [BioLegend]) in permeabilization buffer in the dark and RT. After this step, cells were washed again twice with permeabilization buffer before fixation with BD fixation buffer (1:10 diluted in water). All centrifugation steps were carried out at 4°C with spinning at 450 g for 5 min.

UltraComp beads were used for all compensation controls according to manufacturer instructions, except FVD, where CD4 and CD8 stimulated co-cultures from the corresponding timepoints were used. Fixed cells were analyzed by flow cytometry using either FACS Canto II (BD Biosciences) or Attune NxT (ThermoFisher Scientific) instruments.

Competition/inhibition assay with soluble TAAs and ligands

Pan T cells ($1x10^5$ cells/well) and MOLM-13 cells ($2x10^4$ cells/well) were co-incubated at a 5:1 ratio in RPMI 1640 medium + 10% FBS and 10 µM HSA in round-bottom 96-well plates together with titrations of MP0533 or comparator molecules, with or without competitor molecules (soluble CD33, CD123, CD70, CD27 [AcroBiosystems], and IL-3 [Peprotech]) at a final concentration of 10 nM, 1 nM, or 0.1 nM. Note that the concentrations of soluble TAAs or ligands used in the assay were at least 10-fold higher than those reported in the literature for healthy or diseased individuals (44-46), and for CD123 and CD70 the same concentrations as for CD33 were applied (due to the lack of literature). Cultures were incubated for 48 h at 37°C, 5% CO_2 and then $CD8^+CD25^+$ T-cell activation status was assessed by flow cytometry using FACS Canto II (BD Biosciences) as indicated above. Tumor cell killing was analyzed by lactate dehydrogenase (LDH) release in the supernatants using a cytotoxicity detection kit and according to the manufacturer's instructions (Roche). Overall, competition of CD27, IL-3, and sialic acids for binding of MP0533 to CD70, CD123, and CD33, respectively, was not expected due to the lower affinities of these natural ligands compared to MP0533: binding affinity of CD27 with CD70: K_D ~120-130 nM (47), IL-3 with CD123: K_D ~100-200 nM (and 0.2 nM if βc also present in the complex) (48), sialic acids with CD33: K_D ~0.1-3 mM (49); MP0533 with CD70, CD123 and CD33: K_D ~0.61 nM, 0.056 nM, and 5.1nM, respectively (as reported in Table 1).

Isolation and killing assay with basophils

Basophils and pan T cells were purified from PBMCs of the same donor using negative selection kits (Miltenyi) according to the manufacturer's recommendations. Cells were counted with Luna FL (Logos Biosystems), and then pan T cells were stained with CTV (ThermoFisher Scientific) as described above. CTV-stained pan T cells ($8x10^4$ cells/well) and basophils ($2x10^4$ cells/well) were co-incubated at a 4:1 ratio in RPMI 1640 medium + 10% FBS and 10 µM HSA + 10 ng/ml IL-3 in 96-well plates together with titrations of MP0533 or comparator molecules. Cultures were incubated for 45 h at 37°C, 5% CO_2, and then $CD25^+$ activation status on $CD4^+$ and $CD8^+$ T cells, as well as the percentage of killed basophils were assessed by flow cytometry as described above.

Measurement of cytokines in assay supernatants

For whole blood assays, human fresh blood was collected from anonymous healthy volunteers in accordance with the declaration of Helsinki. TCEs were incubated with whole

blood for 24 h, reduced to 6 h in the presence of MOLM-13 cells due to the higher number of TAA-expressing cells and corresponding higher induction of cytokines. Cytokine release in co-cultures of purified T cells with tumor cells and TCEs was measured after 24 h or 48 h incubation, as indicated throughout the manuscript.

Cytokines in assay supernatants were measured using Meso Scale Discovery (MSD) Multi-Spot Assay System's U Plex Immuno-Oncology Group 1 (Human) kits customized for Granzyme B, IFNγ, IL-2, IL-6, and TNFα quantification. The experiments were performed as directed in the manufacturer's guide. Briefly, supernatants were defrosted at RT and diluted 5-fold before being added to antibody-coated MSD plates. Samples were incubated for 2 h at RT on an orbital shaker at 700 rpm, followed by the addition of detection antibody for an hour again with shaking at RT. Plates were read using MSD MESO QuickPlex SQ. All data files were analyzed using the MSD discovery workbench software and the output values were plotted as non-linear regression graphs using GraphPad Prism (version 9).

Cytokine release and cell count in *ex vivo* whole blood loops

Fresh whole blood was taken from three healthy volunteers and a low amount of soluble heparin was added. The blood was immediately transferred into closed loops followed by administration of the test items, and set to rotate (to mimic the blood circulation) at 37°C to prevent clotting (50). For each donor the same test conditions were analyzed: fresh blood was used for hematology measurements directly after blood collection (baseline value) and then each test condition was sampled at 4, 8 and 24 h after the addition of the test items, with 10 mM EDTA added to each sample to stop the reactions at sampling time points. After each time point, blood samples were analyzed for hematology and flow cytometry, and then processed to plasma for cytokine analysis. Hematology parameters were measured with an XN-L350 analyzer (Sysmex). Cytokines (IFNγ, IL-2, IL-6, TNFα) were measured using the MSD multiplex technology with samples diluted 1:4 and run in duplicates according to the manufacturer's instructions. Data was plotted as area under the curve (AUC) overtime (0-4-8-24 h) values.

hPBMC mouse model xenografted intravenously with MOLM-13 LUC cells

Ten weeks old NXG mice (NOD-*Prkdc*^{scid}-*IL2rg*^{Tm1}/Rj, Janvier) were humanized by i.p. injection of 5x10^6 PBMC prepared from buffy coats in 0.1 ml PBS. After two days, 2x10^5 MOLM-13 LUC cells in 0.1 ml PBS were injected i.v. in the caudal tail vein. Four days after tumor implantation, mice were randomized based on the first imaging timepoint (day 3 after tumor implantation), on PBMC donors and body weight into the different groups of treatment. Treatments with MP0533 or control molecules were initiated five days after tumor implantation (three times per week for MP0533 or daily for CD123-CD3 DART (51) as not half-life extended). Blood was retro-orbitally collected 4 hours after the first treatment for serum isolation and cytokine analysis (performed as described below). Mice were followed until they reached the defined termination time point (day 34 after tumor implantation) or other humane termination criteria (scoring defined in the animal experiment license). Bioluminescence image acquisition was performed using a Newton 7.0 device (Vilber). *In vivo* imaging was performed every 3-4 days starting at day 3 until day 34 post-tumor implantation (10 acquisitions in total). Photos were taken with animals lying on their stomachs, without prior hair removal. Each mouse was injected i.p. with 150 mg/kg of D-luciferin (Promega) in 100 µl PBS 10 min before bioluminescence acquisition, with

aperture set to 0.7. Images were acquired with several exposure times to get images of mice without saturation of the signals. Photon emission per second was then quantified. During bioluminescence acquisitions, mice were anesthetized with a mix of isoflurane and oxygen as a carrier gas. All parameters were analyzed using GraphPad Prism software (version 9.3.1).

hPBMC mouse model xenografted subcutaneously with MOLM-13 cells

NXG mice (NOD-*Prkdc*^{scid}-*IL2rg*^{Tm1}/Rj, Janvier) were humanized by intraperitoneal (i.p.) injection of 5x10^6 PBMC in 0.2 ml PBS. After two days, 10^6 MOLM-13 cells (expressing CD33, CD123, and CD70) or MOLM-13 triple knock-out (KO) cells were injected subcutaneously (s.c.) in a volume of 0.2 ml PBS. Eight days after tumor implantation, mice were randomized, assigned to groups with the same mean tumor volume, and treatment was initiated. To assess efficacy, groups were treated for two weeks by i.v. injections: different doses three times per week for MP0533 (this administration schedule was selected to maintain MP0533 at active concentration within all tested doses, based on the measured MP0533 half-life of 8.0 h determined in MOLM-13 tumor-bearing NXG mice engrafted with human PBMCs) and control DARPins or 0.5mg/kg daily for non-half-life extended CD33-CD3 Bispecific T-cell Engager (BiTE) and CD123-CD3 Dual-Affinity Re-Targeting (DART) molecule as previously reported (51,52)). Tumor growth was then measured 3 times a week with a caliper until a maximum tumor size of 2,000 mm^3 (calculated using length x width x height x π/6) or other termination criteria. Tumors of euthanized mice were collected in formalin. To further dissect the mode of action of MP0533, serum was collected four hours after the first injection to analyze cytokine secretion. Additionally, mice were sacrificed three days after the first injection and blood was collected for validation of humanization by flow cytometry. Serum was also collected to test drug exposure. Tumors were removed and dissociated to assess lymphocyte infiltration/activation (CD8$^+$CD25$^+$CD69$^+$ cells) and TAA expression by flow cytometry. Cytokine release was also quantified in tumor supernatants.

hPBMC mouse model xenografted subcutaneously with RPMI8226 cells

On day 0, NXG mice (NOD-*Prkdc*^{scid}-*IL2rg*^{Tm1}/Rj, Janvier) were xenografted s.c. with 10^7 RPMI8226 cells in a volume of 0.2 ml PBS and then humanized by i.p. injection of 5x10^6 PBMC in 0.2 ml PBS on day 17. On day 22 after tumor implantation, mice were randomized, assigned to groups with the same mean tumor volume, and treatment was initiated. To assess efficacy, groups were treated by i.v. injections: different doses three times per week for MP0533 or 0.5mg/kg daily for non-half-life extended CD33-CD3 Bispecific T-cell Engager (BiTE) as previously reported (52). Tumor growth was then measured with a caliper until day 32 and tumor size was calculated using the formula length x width x height x π/6.

hPBMC subcutaneous xenograft mouse models: sample preparation, acquisition, and analysis

***Single-cell suspension preparation for flow cytometry analyses*.** Mouse blood was harvested in EDTA tubes (SARSTEDT). 100 µL mouse blood was aliquoted in deep 96-well plates and lysed using Fixative-Free Lysing Solution, High-Yield Lyse (ThermoFisher scientific) according to the manufacturer's instructions.

***Tumor dissociation*.** Tumors were cut into small pieces and resuspended in 5 ml dissociation buffer (RPMI 1640 [Gibco], 1/50 Liberase TL [Roche], 1/250 DNase I [Merck]) and processed with a GentleMACS Octo Dissociator (Miltenyi Biotech) to obtain single cell suspensions. The cells were washed in cold PBS and filtered twice through 70 µm and 40 µm cell strainers (Corning). Cell pellets were resuspended in 5 ml DNase I buffer to eliminate cell clumping.

***Staining for flow cytometry*.** Cell pellets were washed by centrifugation at 350 g for 5 min at 4 °C and resuspended in cold Cell Stain Buffer (BD Pharmingen) (0.1 g of tumor in 0.1 ml or 100 µl lysed blood). To reduce Fc receptor-mediated binding by antibodies of interest, single cell suspension samples from each tissue were incubated in Fc block buffer (purified rat anti-mouse CD16/CD32 [BD Biosciences] and purified mouse anti-human CD16/32 [BD Biosciences]) prior to immunostaining. A pre-titrated antibody cocktail including selected markers and TAAs was used to discriminate different immune cell subpopulations and assess their activation, exhaustion, and proliferation state (details in Supplementary Table S4 and Supplementary Table S5), and to evaluate TAA expression on immune and cancer cell populations. Additionally, DARPin binding was determined using an anti-DARPin AF647-conjugated antibody (produced in house).

***Data collection and processing*.** Stained and fixed samples were acquired on the Cytek Aurora full spectral flow cytometer using SpectroFlo acquisition software (version 2.2, Cytek), and data were analyzed with FlowJo (version 10). Samples were unmixed using selected bead and cell-based reference controls. To determine fluorescence spread and identify positively stained cell populations, FMO controls were used for the manual gating. For each gated subpopulation, frequency of the parental population or absolute count of cells (cells/µl) per gate in 0.1 g tumor or 100 µl blood were used for statistical analysis. Expression levels of selected functional markers were evaluated using MFI.

***Detection of cytokine/chemokine levels in humanized mouse sera by Luminex*.** Human cyto-/chemokine levels in humanized mouse sera were measured using a human custom multiplex-4 bead array (R&D Systems) to determine the following cytokines/chemokines: IFN-γ, IL-6, IL-2, and TNF-α according to the manufacturer's recommendations using a Luminex MAGPIX instrument. All test samples were thawed on ice, centrifuged at 2,000 rpm for 3 min, and then diluted 1:2 in a calibrator diluent. Each test sample was assayed as duplicates. In addition, four QC samples were diluted 1:2 in calibrator diluent from various cytokine standard samples in duplicates. Cytokine/chemokine standards supplied by the manufacturer were assayed in duplicates and used to calculate the concentrations of the test samples as well as the QC sample. Cytokine/chemokine levels were measured in serum samples taken 4 h after the first injection.

***Detection of cytokine/chemokine levels in humanized mouse sera by multiplex MSD*.** Human cytokine levels in humanized mouse sera were measured using a human custom multiplex assay (MSD) to determine the following cytokines/chemokines: IL-2, IL-6, IL-8, IL-12p70, IFN-γ, and TNF-α according to the manufacturer's recommendations using a MESO QuickPlex SQ120 instrument. All test samples were thawed on ice, centrifuged at 2,000 rpm for 3 minutes, and then diluted 1:2 in assay diluent 2. Each test sample was measured in duplicates. In addition, four QC samples were diluted 1:2 in assay diluent 2 from four different standard samples (S2, S3, S5, S6) in duplicate on each plate. Cytokine/chemokine standards supplied by the manufacturer were assayed in duplicates and used to calculate the concentration of the test samples as well as the QC samples. Cytokine/chemokine levels were measured in serum samples taken 4 h after the first injection.

***Detection of cytokine/chemokine levels in tumor supernatants by multiplex MSD*.** Human cytokine levels in tumor supernatant were measured using a human custom multiplex assay (MSD) to determine the following cytokines/chemokines: Eotaxin, Granzyme A, Granzyme B, IFN-γ, IL-1α, IL-1β, IL-1RA, IL-2, IL-3, IL-5, IL-6, IL-7, IL-10, IP-10, MCP-1, MIP-1α, MIP-1β, TNF-α (19- or 20-plex), and Rantes (19-plex) or IL-8, IL-12p70 (20-plex) according to the manufacturer's recommendations using a MESO QuickPlex SQ120 instrument. All test samples were thawed on ice and centrifuged at 2,000 rpm for 3 min. Each test sample was measured undiluted in duplicates. In addition, four QC samples were diluted 1:2 in assay diluent 2 from four different standard samples (S2, S3, S5, S6) in duplicate on each plate. Cytokine/chemokine standards supplied by the manufacturer were assayed in duplicates and used to calculate the concentration of the test samples as well as the QC samples. Cytokine/chemokine levels were measured in tumor supernatant samples taken 3 days after the first injection.

CD123 expression on HUVEC

Expression of CD33, CD123, and CD70 was analyzed on HUVEC after 24 h culture under unstimulated, low (0.3 ng/ml TNFα and 1 ng/ml IFNɣ), or high (10 ng/ml TNFα and 10 ng/ml IFNɣ) cytokine (Peprotech) treatment conditions. Cells were washed with PBS and incubated with 100 µl Fc-block (1:100 in PBS; BD Biosciences) for 20 min at 4°C. After an additional wash step with 100 µl PBS, cells were incubated in 100 µl FACS buffer with anti-TAA specific antibodies CD70 (Ki-24), CD123 (6H6), and CD33 (WM53) (all from BioLegend) or isotype controls and LIVE/DEAD fixable cell stain (1:3,000 diluted in PBS; ThermoFisher Scientific) for 30 min at 4°C in the dark. Two wash rounds were then performed, first with 100 µl FACS buffer and then with 200 µl FACS buffer before fixation with BD Fixation Buffer (1:10 diluted in water). All centrifugation steps were carried out at 4°C and 450 g for 5 min. After fixation, cells were analyzed on an Attune Nxt (ThermoFisher Scientific) flow cytometer. Instrument compensation was performed with beads according to the manufacturer's recommendations (ArC Compensation Beads for LIVE/DEAD dye and UltraComp eBeads for labeled antibodies, both from ThermoFisher Scientific).

MP0533 binding to HUVEC

Binding of MP0533 and comparator molecules to HUVEC was assessed after 24 h culture under unstimulated, low (0.3 ng/ml TNFα and 1 ng/ml IFNɣ), or high (10 ng/ml TNFα and 10 ng/ml IFNɣ) cytokine (Peprotech) treatment conditions. Cells were washed with PBS and incubated with 100 µl LIVE/DEAD fixable cell stain (1:3,000 diluted in PBS; ThermoFisher Scientific) for 20 min at 4°C. After an additional wash step, cells were incubated in 100 µl FACS buffer containing 10 µM HSA (CSL Behring) and DARPin or comparator molecules, for 30 min at 4°C. Two wash rounds were then performed, first with 100 µl FACS buffer and then with 200 µl FACS buffer. Next, the cells were incubated for another 30 min with 100 µl/well with either a rabbit anti-DARPin 1.1.1 antibody (2 µg/ml, unlabeled), or FACS buffer for comparator (non-DARPin) molecules. After again two washing steps, 100 µl/well goat anti-rabbit IgG (for detection of DARPins) (ThermoFisher Scientific), goat-anti human IgG (for detection of CD123-CD3 ADAPTIR) (ThermoFisher Scientific), or mouse anti-Penta His (for detection of CD33-CD3 BiTE and CD123-CD3 DART) (Qiagen) antibodies (1:1000 diluted in FACS buffer) were added to wells. After subsequent incubation at 4°C for 20 min, cells were again washed twice with FACS buffer and finally fixed with BD Biosciences Fixation Buffer

(1:10 diluted in water). All centrifugation steps were carried out at 4°C and 450 g for 5 min. After fixation, cells were analyzed on an Attune Nxt (ThermoFisher Scientific) flow cytometer. Instrument compensation was performed with beads according to the manufacturer's recommendations (ArC Compensation Beads for LIVE/DEAD dye and UltraComp eBeads for labeled antibodies, both from ThermoFisher Scientific).

HUVEC killing assay

HUVEC were thawed 5 days before the experiment and cultured at 37°C, 5% CO_2 in EGM-2 (Lonza) supplemented with 5% FBS, 10 µM HSA, and the following supplement mix (Promocell): ascorbic acid, heparin, recombinant human FGF-B, EGF, hydrocortisone, and VEGF. Culture medium was then substituted for medium containing either low (0.3 ng/ml TNFα and 1 ng/ml IFNɣ) or high (10 ng/ml TNFα and 10 ng/ml IFNɣ) cytokine (Peprotech) treatment for additional 24 h (unstimulated cells were used to assess baseline TAA expression). HUVEC were collected using Accutase (Innovative Cell Technologies), washed, and resuspended in PBS for the subsequent Cytolight rapid red labeling (Sartorius) according to the provided protocol. HUVEC (final 10,000 per well) were seeded in a 96-well flat bottom plate and incubated for 4 h until adherent. Once HUVEC were adherent, 50,000 purified and freshly thawed human pan T cells were added to the wells (E:T ratio 5:1) in assay medium containing 1 mM $CaCl_2$ and Annexin V green (final dilution 1/200; Sartorius), followed by serial dilutions of selected DARPin, comparator, or control proteins in duplicates. Assay medium also contained 10 µM HSA. The co-culture was incubated for 48 h in an IncuCyte S3 (Sartorius) and the wells scanned in red and green channels every 3 h (10x magnification) to identify living vs. apoptotic HUVEC (respectively). Exported values were analyzed and plotted using GraphPad Prism software (version 9).

Ex vivo autologous killing assay with fresh bone marrow of AML patients

Fresh bone marrow samples from adult patients with AML (see Supplementary Table S6 for details) were collected in tubes containing heparin as an anticoagulant, at the respective hospital centers within the patient's regular treatment schemes, following clinical practice at the center. A fraction of the extracted sample, together with the signed patient's informed consent, was sent to the laboratory under Center's Ethical Committees approved research study protocols.

As previously described (53), a fraction of the sample was stained with specific monoclonal antibodies (mAbs) to identify pathological cells and determine cell viability. The combination of mAbs used for the initial evaluation of each sample included anti-human CD34, CD117, CD45, CD5, CD25, CD64, HLADR, together with Annexin V. Each sample was then diluted 1:5 in appropriate volume of IMDM/L-Glutamine 4 mM, supplemented with 20% FBS and 1% antibiotics to a final volume of 60 µL per well containing the pathological cells (the number of pathological cells depended on the infiltration of the sample). The mixture containing the cells was dispensed into 96-well plates containing 60 µl of compounds, previously prepared using an automated Echo 550 liquid handler (Labcyte). The plates were incubated for 48 and 120 h at 37°C in humidified atmosphere containing 5% CO_2. At final endpoints and after the supernatants were collected, red blood cells were lysed, and the remaining cells were stained with Annexin V and the mAbs that better discriminated pathological cells according to baseline characterization. Parameter estimation was performed by an individual modeling approach to dose-response experiments. The used

model to fit the data was a single-dose-response inhibitory logistic model based on the Hill equation (see equation below), where the dependent variable analyzed was the number of live cells of a particular population counted by the cytometer at every tested concentration of drug.

$$Y = E_0 \times \left[\frac{E_{max} - E_0}{1 + 10^{(C-x)*D}}\right]$$

Concentration data points were input as $\log_{10}$ transformation and were fitted using the Levenburg Marquardt algorithm with the Xlfit software package by IDBS. For a more comprehensive interpretation of results, a normalization was done where an independent variable was referenced to the basal parameter value from each curve fitted using cell count.

Primary LSC and HSC killing and clonogenicity assay

For colony-forming unit (CFU) assays only AML samples that contained between 50-80% tumor cells and displayed a $CD34^+$ immunophenotype were used. Furthermore, only AML samples were used where the previous analysis of the variant allele frequency of mutations unrelated to CHIP (clonal hematopoiesis of indeterminate potential) in colony assays indicated the growth of leukemia cells.

TAA expression on AML (peripheral blood or bone marrow, Supplementary Table S7) and healthy donor bone marrow samples was assessed by flow cytometry of $CD34^+$ LSC and HSC cells (gated as $CD45^{dim}Lineage^-CD90^-CD34^+CD38^{+/-}$) using anti-human CD70 (Ki-24), CD123 (6H6), and CD33 (WM53) monoclonal antibodies (BioLegend) as shown in Supplementary Fig. S5. MFI values were exported from FlowJo (version 10) (individual values in Supplementary Table S8) and plotted using GraphPad Prism software (version 9).

Sorted $CD45^{dim}Lin^-CD90^-CD34^+$ AML (2,000 to 50,000 cells/well) or healthy donor (500 cells/well) cells were co-cultured at an effector to target (E:T) ratio of 1:1 with allogeneic pan T cells and treated with the indicated compounds and concentrations for four days in 96-well U-bottom plates in StemSpan SFEM medium containing a cytokine mix (StemSpan CC100, containing SCF, IL-6, IL-3, and Flt3L; all STEMCELL Technologies) and in the presence of 10 µM HSA. After incubation, cells were transferred into cultivation medium containing cytokines and 1.27% methylcellulose to assess the colony-forming capacity for each condition. After 14 days additional culture colonies were counted by light microscopy.

Assessment of LSC killing *in vivo*

Fresh $CD45^+CD34^+$ human AML PDX (Supplementary Table S7) cells were isolated from bone marrow of NSG mice by magnetic depletion of mouse cells (Mouse Cell Depletion Kit, CD45-specific, Miltenyi) following the manufacturer's recommendations, and then 10^6, 10^5, 10^4, or 10^3 cells/well were co-cultured at an E:T ratio of 1:1 with allogeneic pan T cells and 10 pM of indicated compound in triplicate as described above. After 2 days of incubation, cells were pooled by treatment, and OKT3 antibody was added at 1 µg/10^6 cells to allow depletion of human T cells once injected into mice (54). NSG mice (NOD.Cg-Prkdc^{scid} Il2rg^{tm1Wjl}/SzJ, Charles River Laboratories) were sub-lethally irradiated with 150 cGy, randomized in 3 animals/group, and injected i.v. the same day with each cell concentration. Engraftment was monitored in blood by staining for human $CD45^+CD34^+$ cells, and the experiment terminated once the disease was successfully established (9 weeks for PDX1 and

15 weeks for PDX2). Bone marrow, spleen, and blood were collected and stained for $hCD45^+CD34^+$ for cell identification and CD33, CD123, and CD70 (as described above) for TAA expression analysis at termination. Both engraftment and TAA expression were analyzed by flow cytometry. Additionally, to assess colony-forming capacity, 20,000 whole bone marrow cells from each NSG mouse were cultivated in medium containing cytokines and 1.27% methylcellulose for 14 days and counted as above. Statistical significance was calculated using the Extreme Limiting Dilution Analysis (ELDA) software (55).

Combination of MP0533 with azacitidine and venetoclax

CTV-labeled pan T cells ($1.5x10^4$ cells/well) and MOLM-13 cells ($1.5x10^4$ cells/well) were co-incubated at 1:1 ratio (generally used for experiments lasting 72 h or longer, while up to 5:1 was used for experiments performed within 48 h) in RPMI 1640 medium + 10% FBS and 10 µM HSA in round-bottom 96-well plates with titrations of MP0533, azacitidine (Aza), or venetoclax (Ven). Killing EC50s for each compound after 72 h incubation were determined by tumor cell count and calculated using Graph Pad Prism (version 9). Combination of MP0533 with Aza and/or Ven was then assessed by repeating the same killing assay with EC50 concentrations of each compound vs. 2-fold incremental/decremental titrations. Synergy, based on the Chou-Talalay method (56,57), was calculated using the CompuSyn software (58) by assessing combination index (CI) and fraction affected (FA) values, with CI values <1 indicating synergism, =1 additive effect, >1 antagonism.

Additionally, combination of MP0533 with Aza/Ven at EC50 concentrations was also assessed on primary AML $CD34^+$ sorted LSCs (25). Briefly, AML samples (PBMC or BMMC) were flow-sorted for $CD45^{int}Lin^-CD90^-CD34^+$ cells and then co-cultured at an E:T ratio of 1:1 with PBMC-purified allogenic pan T cells and treated with 10 pM MP0533 or control NB-CD3 DARPin ± 1 µM Aza and 5 nM Ven for four days in round-bottom 96-well plates in StemSpan SFEM medium containing a cytokine mix (StemSpan CC100, containing SCF, IL-6, IL-3, and Flt3L; STEMCELL Technologies) and in presence of 10 µM HSA. After incubation, cells were transferred into cultivation medium containing cytokines and 1,27% methylcellulose to assess colony forming capacity for each condition. Colonies were counted after 14 days additional culture by light microscopy and plotted using GraphPad Prism (version 9).

Data availability

The data generated in this study are available within the article and its Supplementary Data files or upon request from the corresponding author.

Results

Design of the multispecific DARPin molecule MP0533

MP0533 consists of a single polypeptide chain, comprising six DARPin domains: two N-terminal anti-HSA domains for *in vivo* half-life extension (38); three domains that specifically bind to TAAs CD33, CD123, and CD70; and a C-terminal CD3-binding domain for T-cell engagement. The selection of the final format (Figure 1A) with optimized efficacy and safety is described in detail in the Materials and Methods section and Supplementary Fig. S1.

MP0533 binding affinities

SPR measurements showed binding of MP0533 to human CD33, CD123, and CD70 with affinities of 5 nM, 0.06 nM, and 0.6 nM, respectively (Table 1, Supplementary Fig. S2A). Lower binding affinities were measured on human CD3 and HSA, with 24 nM and 120 nM, respectively. More specifically, the anti-CD3 DARPin, with its double-digit nM affinity against CD3, was selected for optimal activity vs. safety (59). The HSA-binding DARPin in MP0533 has also been used in other clinical-stage DARPins (eg MP0317 or MP0310) and is cross-reactive to mouse serum albumin. No cross-reactivity to target mouse proteins other than serum albumin was observed.

In addition, the simultaneous binding of MP0533 to HSA, CD33, CD123, CD70, and CD70 was also demonstrated by SPR (Supplementary Fig. S2B).

MP0533 shows preferential killing of tumor cells expressing combinations of TAAs

Exploiting the principle of avidity, MP0533 was engineered for enhanced binding to cells that co-express two or three TAAs, thereby intensifying T cell–mediated cytotoxicity against these cells. To validate this, we assessed MP0533 in potency assays in the presence of healthy allogeneic T cells and engineered MOLM-13 tumor cell lines expressing one, two, or all three TAAs (Supplementary Fig. S6). Figure 1B shows similar dose-dependent activation of $CD8^+$ T cells and killing of MOLM-13 cells expressing ≥2 TAAs (red and orange curves, half maximal effective concentrations [EC50s] of 8-27 pM and 10-46 pM for T-cell activation and cell killing, respectively), while an approximate 10-fold lower potency was measured on cells expressing a single TAA (green curves, EC50s of 38-431 pM and 107-457 pM for T-cell activation and cell killing, respectively) (all values in Supplementary Table S9). TAA-specific binding of MP0533 to MOLM-13 cell lines and CD3-specific binding to T cells are shown in Supplementary Fig. S7.

MP0533 induces killing of AML cell lines with limited release of cytokines

MP0533 activity in situations of tumor heterogeneity was modeled by performing additional tumor cell killing assays with various AML cell lines expressing different TAA levels (Supplementary Fig. S8). As shown in Figure 1C, MP0533 induced killing of all cell lines tested, with EC50s ranging from 3 to 60 pM. Also, when compared to other TCEs, at equal efficacious dose (equal % of cell killing), MP0533 showed reduced release of cytokines in supernatants (Figure 1D) without impaired production of the cytotoxic granule protein granzyme B, suggesting a more favorable therapeutic window for MP0533. While other TCE comparators were also inducing lower levels of cytokines than CD123-CD3 DART, the levels measured for MP0533 were constantly the lowest, including for IL-6, considered a key cytokine in the manifestation of cytokine release syndrome (CRS) events (60).

Additionally, the kinetics of T-cell activation were not different between MP0533 and other TCEs: T-cell activation, proliferation, and cytotoxic markers were all similar among the tested molecules (Supplementary Fig. S9).

MP0533 activity is not inhibited by the presence of soluble TAAs or natural ligands

We checked the potential influence of soluble TAAs or natural ligands (IL-3 for CD123 and CD27 for CD70) and found that none interfered with MP0533 activity (Supplementary

Fig. S10). Only the simultaneous presence of all three soluble TAAs at supraphysiological concentrations led to a reduced potency in T-cell activation and tumor cell killing assays, but we consider such a condition to be non-physiological: while IL-3, soluble CD27, and soluble CD33 can be measured in serum of healthy and/or diseased individuals (44-46), no data on soluble CD123 or CD70 could be found in the literature, suggesting that both CD123 and CD70 are either not shed or not found at detectable or relevant concentrations.

MP0533 induces tumor regression and is well tolerated in hPBMC mouse xenograft models

As MP0533 binds to human TAAs on human immune and AML cells but not their murine orthologs, *in vivo* pharmacodynamic (PD) activity was demonstrated in xenograft models in which human AML tumors were grown in immune-suppressed NXG mice implanted with PBMCs from healthy human donors before the xenograft of human AML cancer cells.

In the first study, mice were grafted s.c. with MOLM-13 tumors expressing the three TAAs targeted by MP0533 (Figure 2A). A dose-dependent antitumor activity of MP0533 and comparator TCEs against MOLM-13 tumors is shown in Figure 2B. This correlated with the induction of T-cell activation in the tumors (Figure 2C) in the absence of significant T-cell activation in the blood. In addition, MP0533 did not induce systemic cytokine release 4 h after the first dose while the CD123-CD3 DART comparator induced the release of a broad range of human cytokines (Figure 2D) into the blood. Analysis of tumors harvested 3 days after treatment initiation (after 2 doses of MP0533 or comparator molecules) showed that the highest dose of MP0533 and the CD123-CD3 DART comparator induced human cytokine release in the tumors (Figure 2E), correlating with tumor regression. In a similar model, MP0533 efficacy was also demonstrated *in vivo* against s.c. RPMI8226 tumors (Supplementary Fig. S11). RPMI8226 cells are CD33- and CD123-expressing cells, but with very low expression of CD70 (Supplementary Fig. S8), more closely mimicking the expression profile found on primary AML cells.

The specificity of MP0533 for tumors expressing the three targeted TAAs was then demonstrated in a study that compared MP0533 activity in NXG mice xenografted s.c. with both MOLM-13 wild-type (WT) tumors expressing CD33, CD123, and CD70 and MOLM-13 triple KO tumors (KO for CD33, CD123, and CD70) (Supplementary Fig. S12A). MP0533 demonstrated TAA-specific antitumor activity against MOLM-13 WT tumors while MOLM-13 KO tumors were not significantly affected (Supplementary Fig. S12B). This activity correlated with the observation that MP0533 induced T-cell activation and cytokine/chemokine release only in MOLM-13 WT tumors (Supplementary Fig. S12C and D). MP0533 did not induce systemic T-cell activation in the blood (Supplementary Fig. S12F). Similarly to MP0533, CD33-CD3 BiTE also showed activity against MOLM-13 WT tumors only (Supplementary Fig. S12B), but cytokine/chemokine release (Supplementary Fig. S12E) and T-cell activation (Supplementary Fig. S12F) were also detected systemically in the blood and in MOLM-13 KO tumors (Supplementary Fig. S12C and D). Rather than caused by a direct unspecific activity of CD33-CD3 BiTE against the MOLM-13 KO tumors, our data suggest that the cytokines found in the KO tumors were the consequence of a higher infiltration of systemically activated human T and $CD33^+$ cells (Supplementary Fig. S12E-G), the latter also potentially acting as target in the KO tumors.

Potent MP0533 activity *in vivo* was additionally demonstrated in NXG mice xenografted i.v. with MOLM-13 LUC cells to produce disseminated tumor growth (Figure 3A).

MP0533 inhibited the growth of tumor cells at all tested doses (Figure 3B-D). Comparable antitumor activity to that of the lowest dose of MP0533 (0.02 mg/kg every 3 days) was produced by the CD123-CD3 DART comparator dosed daily at 0.5 mg/kg, which also induced significant release of cytokines 4 hours after treatment. MP0533 showed no significant increases in cytokines (Figure 3E) and, similarly to CD123-CD3 treated mice, no significant body weight loss (Supplementary Fig. S13), indicating that MP0533 induced dose-dependent antitumor activity while being well tolerated.

MP0533 induces low levels of cytokine release *ex vivo* in blood

By limiting on-target, off-tumor effects, MP0533 has the potential to reduce dose-limiting toxicities, such as CRS and the hematological toxicities often observed in clinical development with potent bispecific TCEs and chimeric antigen receptor (CAR) T-cell therapies (17). We assessed the impact of MP0533 on cytokine release and healthy blood cells with different *ex vivo* healthy whole blood assays.

When incubated in rotating whole blood loops, MP0533 induced only minimal release of cytokines and decrease of white blood cell (WBC) or platelet counts compared to the CD123-CD3 DART and CD33-CD3 BiTE molecules, as shown in Figure 4A and B (and Supplementary Fig. S14) as area under the curve (AUC) over 24 h incubation. For MP0533, the decrease in WBC counts appears to be driven only by decreases in monocytes, whereas for the other TCEs, lymphocytes, granulocytes as well as monocytes decreased. Reduction in platelet counts was likely caused by indirect effects related to effects on WBCs. Red blood cell counts were not affected by any of the molecules.

Cytokine release in healthy whole blood was also measured in plate-based assays, either in the absence (Figure 4C) or presence of MOLM-13 cells to mimic a diseased status with about 20% AML blast content (Figure 4D) after 24 or 6 h incubation, respectively. Again, with both setups, we saw a marked reduction of cytokine release with MP0533 compared to competitor TCEs.

Overall, these results show that MP0533 did induce the release of cytokines, a hallmark of T-cell activation, but with 14- and 5-fold lower AUC and 8- and 3-fold lower c-max levels than CD123-CD3 DART and CD33-CD3 BiTE comparator molecules, respectively (calculated as average of median cytokine AUCs or c-max values across all measurements shown in Figure 4).

MP0533 shows a favorable on-target, off-tumor profile

Overall, no major impact of MP0533 on white blood cells and platelets (Figure 4B), or lymphocytes, monocytes, and neutrophils (Supplementary Fig. S14), was observed when assessed in whole blood loops over 24 h, while decreased cell counts were observed with both CD33-CD3 BiTE and CD123-CD3 DART comparator molecules. However, effective targeting of basophils, the highest TAA co-expressing (CD123 and CD33, Supplementary Fig. S3B-C) non-tumoral cells, was shown *ex vivo* by the activation of autologous T cells and killing of basophils when co-cultured with MP0533 or comparator CD123 or CD33 targeting TCEs (Figure 5A).

T-cell fratricide has been reported with a potent CD70-specific TCE (61), as CD70 is upregulated on activated T cells so can become a target on effector cells (62,63). Therefore, we assessed potential MP0533-induced killing of T cells in co-culture with MOLM-13 cells and did not find any impact on $CD4^+$ and $CD8^+$ T-cell viability or count/proliferation (Figure

5B), and no difference vs. the non-CD70 targeting TCEs CD123-DART (also shown in Supplementary Fig. S15) and CD33-BiTE.

CD123, expressed on endothelial cells (64) and further upregulated under inflammatory conditions (65), can become a safety concern with CD123-targeted therapies, where capillary leak syndrome (CLS) has been reported (as shown for tagraxofusp (66,67)). To assess the effects of MP0533 on endothelial cells, we measured T cell–mediated killing of HUVEC previously stimulated with IFNγ and TNFα to induce expression of CD123 (to mimic inflammatory status, see Supplementary Fig. S16A, top panels). Figure 5C shows that MP0533, despite binding to the cells (Supplementary Fig. S16A and B), did not induce the killing of HUVEC, even with over-expressed CD123. In contrast, the CD123-CD3 targeting DART molecule effectively killed CD123-expressing HUVEC. The CD33-CD3-targeting BiTE showed no killing (or binding) of HUVEC, confirming that potential off-tumor targeting of endothelial cells is not CD33-mediated.

These data, together with the absence of T-cell fratricide, support the hypothesis that MP0533 has a low capacity to induce cell killing when only a single TAA is expressed on target cells.

MP0533 induces killing of primary AML blasts and is selective for LSCs

MP0533 activity was analyzed in five primary AML bone marrow samples, from 2 newly diagnosed and 3 previously treated patients with different TAA expression/co-expression levels and E:T ratios (from 10:1 to 1:28). Fresh bone marrow samples were diluted into assay medium without prior purification of cells and incubated for 48 and 120 h with serial dilutions of MP0533 or comparator molecules. Figure 6A shows that MP0533 induced T-cell activation (left panel), proliferation (right panel, black curves), and tumor cell killing (right panel, red curves) with similar kinetics and efficacy to the more potent CD123-CD3 DART and CD33-CD3 BiTE molecules. These data show that MP0533 could successfully induce both activation of patient autologous T cells and killing of tumor cells presenting very different levels of TAAs (CD33: ≈200-8,000 molecules/cell; CD123: ≈500-2,500 molecules/cell, CD70: at limit of quantification), the latter supporting the hypothesis that the multitargeting approach of MP0533 has the potential to counteract tumor heterogeneity in AML patients.

We further addressed LSC killing and specificity in a cell killing and colony-forming assay with $CD34^+$ sorted AML (LSC) and healthy donor (HSC) cells. Co-cultures of LSCs with allogeneic T cells in the presence of MP0533 resulted in a dose-dependent reduction in colony formation, with almost no CFUs being detected at the highest DARPin concentration of 1,000 pM (Figure 6B, left panel). The comparator molecules CD33-CD3 BiTE and CD123-CD3 DART showed a higher efficacy in inhibiting LSC colony-forming capacity at lower concentrations (i.e. higher potency, as seen on MOLM-13 cell line, Figure 1D). However, MP0533 only marginally affected colony formation of normal HSCs, while both comparator molecules substantially reduced the clonogenic potential of normal HSCs in a dose-dependent manner. Moreover, as CD70 expression was close to the limit of detection by flow cytometry for most LSC samples (Figure 6B, right panel), we also addressed whether CD70 is an effective target for a TCE on LSCs by using a single-targeting CD70-CD3 DARPin control molecule. As shown in Figure 6B, such a molecule was also able to reduce CFUs of LSCs, while HSCs were unaffected, confirming that CD70 is indeed a selective target on LSCs (as previously reported (46)).

The ability of MP0533 to induce killing of LSCs was additionally confirmed *in vivo*. AML PDX samples were first co-incubated *ex vivo* with MP0533 and allogeneic T cells, and then injected in sub-lethally irradiated NSG mice to assess residual engraftment capacity. As shown in Figure 6C (left panel), treatment with MP0533 at an EC50 concentration of 10 pM resulted in a ≥10-fold ($p<0.05$ for both PDX samples) reduction of engraftment in mice compared to the non-TAA binding (NB-CD3) control DARPin (see also Supplementary Fig. S17 for TAA expression analysis on PDX1 cells at endpoint). The difference between MP0533 and CD123-CD3 DART was not significant. In addition to engraftment *in vivo*, the presence of LSCs in engrafted mice was also assessed by subsequent cultivation of isolated bone marrow cells *ex vivo.* Colony counts after 14 days of culture (Figure 6C, right panel) confirmed a >10-fold reduction of LSCs after treatment with MP0533, compared to the NB-CD3 control DARPin.

MP0533 activity is increased in combination with azacitidine/venetoclax

Finally, we addressed a potential treatment combination in co-culture killing assays with primary AML $CD34^+$ LSCs (confirmed on MOLM-13 cells) and allogeneic T cells. Synergy was observed when MP0533 was used together with azacitidine and venetoclax (treatments commonly used and indicated in the US for newly diagnosed AML patients aged ≥ 75 years or with co-morbidities that preclude the use of intensive induction chemotherapy) at sub-optimal (EC_{50}) doses (Supplementary Fig. S18).

Altogether, data collected on primary cells show that MP0533 is efficacious in engaging patient T cells, inducing the killing of AML tumor cells as well as effectively eliminating LSCs while sparing HSCs, and has synergistic effect in combination with azacitidine and venetoclax.

Discussion

Despite treatment progress made in recent years, the prognosis for AML remains poor. The disease is mainly driven by LSCs that resist conventional chemotherapy and are the primary cause of relapse (7,13,14). Additionally, aberrant proliferation, symmetric self-renewal, increased survival, and defective differentiation of malignant blasts are other key oncogenic drivers in AML.

The development of targeted immunotherapy treatments is challenging due to both the lack of AML-specific target antigens and clonal heterogeneity of the disease (15). Agents targeting single antigens on tumor cells have been assessed in the clinic but only gemtuzumab ozogamicin, a CD33-targeted ADC, was approved (68). More recently investigated agents include TCEs (like the CD123-targeted DART flotetuzumab (22) and the CD33-targeted BiTE AMG330 (19)) and CAR T cells (69-71). However, clinical development of both TCEs has been stopped also due to limited therapeutic indices. Nevertheless, non-clinical versions of the two were included in the studies reported here as efficacy and safety comparators.

Despite numerous attempts to identify specific cell surface markers on AML cells that might overcome the problems identified to date with single targeted agents (72,73), none has been found so far. We propose here an innovative approach involving combinatorial targeting of different validated TAAs on AML cells and LSCs (16,17) to enhance the therapeutic efficacy, reduce toxicity, and address TAA expression heterogeneity both within and between patients. MP0533 is a CD3-binding T-cell engaging DARPin that can bind

simultaneously to three AML antigens: CD70, CD33, and CD123 as well as to HSA to extend the circulatory half-life of the molecule. Optimal binding affinity to each target was engineered to enable an avidity-like selectivity to facilitate preferential T cell–mediated killing of AML cells co-expressing at least two of these TAAs, while sparing non-tumor cells expressing single TAAs.

In the presented *in vitro* studies, MP0533 achieved the desired selectivity against AML cells co-expressing at least two targets, while cells expressing single TAAs are killed only at 10-fold higher concentrations. Moreover, efficacy of MP0533 on all tested AML cell lines showed that MP0533 can tolerate target expression heterogeneity: its potency depending on the number of different TAAs expressed rather than on the level of expression of each single TAA. This correlates with previous findings that showed absence of association between CD123 or CD33 expression and cytotoxicity induced by the TCEs flotetuzumab (22) and AMG330 (74), respectively. This was confirmed in *ex vivo* studies with primary bone marrow samples from different AML donors, where activation of autologous T cells led to the killing of AML blasts having different TAA expression levels (and co-expression profiles). Importantly, MP0533 showed a preferential targeting of LSCs compared to HSCs. Effective targeting of LSCs was also demonstrated by the reduced engraftment *in vivo* of $CD34^+$ PDX cells after *ex vivo* treatment with MP0533. Samples from patients with 50-80% tumor burden and showing variant allele-frequency of mutations indicating the growth of leukemia cells were used for CFU assays with $CD34^+$ AML cells. Based on these selections, we can assume that the effect on CFU observed in our assays was caused by the reduction in AML LSCs rather than in remaining normal hematopoietic stem and progenitor cells. Additionally, similar efficacy in both autologous and allogeneic settings and the lack of cytotoxicity with TAA- or CD3-missing control DARPins suggest that the effect of HLA mismatch was negligible in our data.

Mouse antitumor studies complemented the *in vitro* and *ex vivo* findings. The *in vivo* activity of MP0533 was demonstrated in humanized mice xenografted s.c. with human MOLM-13 tumors. MP0533 induced dose-related antitumor activity as well as T-cell activation and cytokine release in the tumors. T-cell activation and cytokine release were not observed in the blood. Comparable PD activity was seen in the tumors by a CD33-CD3 BiTE and a CD123-CD3 DART but, in contrast to MP0533, these agents also activated T cells and induced cytokine and chemokine release systemically. MP0533 antitumor function was also demonstrated in a mouse tumor model expressing lower levels of TAAs (RPMI8226) and was shown to be TAA-dependent, having no effect on the growth of MOLM-13 triple KO tumors. Finally, the dose-dependent antitumor activity of MP0533 was confirmed in a tumor model closer to leukemia, where MOLM-13 cells were xenografted i.v. to produce disseminated tumor growth.

A finding across all studies was that cytokine release was markedly lower at active concentrations of MP0533 than was observed with TCEs targeting single TAAs (CD123-CD3 DART and CD33-CD3 BiTE), suggesting that MP0533 may be better tolerated with respect to CRS than has been reported for other agents in clinical development for AML patients (22,75). Our data show that the geometry and format of MP0533 are linked to its lower cytokine secretion profile vs. other TCEs. However, the format of the different TCEs, affinities to the TAAs and CD3, epitopes, and the derived immunological synapse are likely also contributing to the different profiles observed.

With respect to safety, the presented data indicate that MP0533 may also have a lower propensity than single-targeting TCEs to induce CD70-dependent T-cell fratricide (61)

or CLS (66,67) due to on-target, off-tumor effect on endothelial cells activated under cytokine-induced inflammatory conditions to express CD123 (64,65).

In conclusion, these studies demonstrated that the intended avidity-driven PD activity of MP0533 resulted in a favorable therapeutic window, as shown by the increased selective T cell-mediated killing of AML cells and LSCs vs. HSCs. Further, this selective T cell-mediated killing resulted in significantly lower cytokine and chemokine release than is seen with single TAA targeting TCEs. Collectively, our data suggest that the tolerance of MP0533 to expression heterogeneity and its selective activity could translate into deeper and more durable responses in the clinic.

The multitargeting approach adopted with MP0533 has the potential to bring a new therapeutic option to patients with high unmet need, principally older or unfit patients. At the time of writing, a phase 1, first-in-human, open-label, multicenter, dose-escalation study (NCT05673057) evaluating the safety, tolerability, and efficacy of MP0533 is ongoing in patients with relapsed/refractory AML. The study additionally includes a range of secondary endpoints, like the effect on LSCs, T-cell activation, cytokine release, and pharmacokinetics.

Authors' Contributions

M. Bianchi: conceptualization, investigation, methodology, formal analysis, visualization, supervision, writing – original draft, writing – review & editing. **C. Reichen:** conceptualization, methodology, formal analysis, visualization, supervision, writing – original draft. **A. Croset:** conceptualization, methodology, formal analysis, visualization, supervision, writing – original draft. **S. Fischer:** investigation. **A. Eggenschwiler:** investigation. **Y. Grübler:** investigation. **R. Marpakwar:** investigation. **T. Looser:** investigation. **P. Spitzli:** investigation. **C. Herzog:** investigation. **D. Villemagne:** investigation. **D. Schiegg:** investigation. **L. Abduli:** investigation. **C. Iss:** investigation. **A. Neculcea:** investigation. **M. Franchini:** investigation, methodology, formal Analysis. **T. Lekishvili:** investigation, formal analysis, visualization. **S. Ragusa:** investigation, formal analysis, visualization. **C. Zitt:** methodology, formal analysis. **Y. Kaufmann:** investigation. **A. Auge:** investigation. **M. Hänggi:** investigation. **W. Ali:** investigation. **T. M. Frasconi:** investigation, formal analysis, visualization. **S. Wullschleger:** methodology, formal analysis. **I. Schlegel:** investigation. **M. Matzner:** investigation. **U. Luethi:** investigation. **B. Schlereth:** conceptualization, methodology, supervision. **K. M. Dawson:** methodology, writing – original draft. **V. Kirkin:** project administration, writing – review & editing. **A. F. Ochsenbein:** supervision, writing – review & editing. **S. Grimm:** conceptualization, methodology, supervision. **N. Reschke:** conceptualization, methodology, supervision. **C. Riether:** conceptualization, methodology, supervision, writing – review & editing. **D. Steiner:** resources, supervision, writing – review & editing. **N. Leupin:** conceptualization, resources, supervision, writing – review & editing. **A. Goubier:** conceptualization, resources, supervision, writing – review & editing.

Acknowledgements

The authors thank Joanna Robinson, Marcela Guzman Ayala, and Kenneth Crook from Molecular Partners AG, Schlieren, Switzerland, for their critical input and proofreading of the manuscript.

References

1. Stone RM, Mandrekar SJ, Sanford BL, Laumann K, Geyer S, Bloomfield CD*, et al.* Midostaurin plus Chemotherapy for Acute Myeloid Leukemia with a FLT3 Mutation. N Engl J Med **2017**;377:454-64
2. Roboz GJ, DiNardo CD, Stein EM, de Botton S, Mims AS, Prince GT*, et al.* Ivosidenib induces deep durable remissions in patients with newly diagnosed IDH1-mutant acute myeloid leukemia. Blood **2020**;135:463-71
3. Maiti A, Qiao W, Sasaki K, Ravandi F, Kadia TM, Jabbour EJ*, et al.* Venetoclax with decitabine vs intensive chemotherapy in acute myeloid leukemia: A propensity score matched analysis stratified by risk of treatment-related mortality. Am J Hematol **2021**;96:282-91
4. Wei AH, Montesinos P, Ivanov V, DiNardo CD, Novak J, Laribi K*, et al.* Venetoclax plus LDAC for newly diagnosed AML ineligible for intensive chemotherapy: a phase 3 randomized placebo-controlled trial. Blood **2020**;135:2137-45
5. Roboz GJ, Montesinos P, Selleslag D, Wei A, Jang JH, Falantes J*, et al.* Design of the randomized, Phase III, QUAZAR AML Maintenance trial of CC-486 (oral azacitidine) maintenance therapy in acute myeloid leukemia. Future Oncol **2016**;12:293-302
6. Sasaki K, Ravandi F, Kadia TM, DiNardo CD, Short NJ, Borthakur G*, et al.* De novo acute myeloid leukemia: A population-based study of outcome in the United States based on the Surveillance, Epidemiology, and End Results (SEER) database, 1980 to 2017. Cancer **2021**;127:2049-61
7. Craddock C, Quek L, Goardon N, Freeman S, Siddique S, Raghavan M*, et al.* Azacitidine fails to eradicate leukemic stem/progenitor cell populations in patients with acute myeloid leukemia and myelodysplasia. Leukemia **2013**;27:1028-36
8. Dombret H, Seymour JF, Butrym A, Wierzbowska A, Selleslag D, Jang JH*, et al.* International phase 3 study of azacitidine vs conventional care regimens in older patients with newly diagnosed AML with >30% blasts. Blood **2015**;126:291-9
9. Kantarjian HM, Thomas XG, Dmoszynska A, Wierzbowska A, Mazur G, Mayer J*, et al.* Multicenter, randomized, open-label, phase III trial of decitabine versus patient choice, with physician advice, of either supportive care or low-dose cytarabine for the treatment of older patients with newly diagnosed acute myeloid leukemia. J Clin Oncol **2012**;30:2670-7
10. Gallazzi M, Ucciero MAM, Faraci DG, Mahmoud AM, Al Essa W, Gaidano G*, et al.* New Frontiers in Monoclonal Antibodies for the Targeted Therapy of Acute Myeloid Leukemia and Myelodysplastic Syndromes. Int J Mol Sci **2022**;23
11. Abaza Y, Fathi AT. Monoclonal Antibodies in Acute Myeloid Leukemia-Are We There Yet? Cancer J **2022**;28:37-42
12. Khaldoyanidi SK, Hindoyan A, Stein A, Subklewe M. Leukemic stem cells as a target for eliminating acute myeloid leukemia: Gaps in translational research. Critical reviews in oncology/hematology **2022**;175:103710
13. van Gils N, Denkers F, Smit L. Escape From Treatment; the Different Faces of Leukemic Stem Cells and Therapy Resistance in Acute Myeloid Leukemia. Front Oncol **2021**;11:659253
14. Zeng Z, Shi YX, Samudio IJ, Wang RY, Ling X, Frolova O*, et al.* Targeting the leukemia microenvironment by CXCR4 inhibition overcomes resistance to kinase inhibitors and chemotherapy in AML. Blood **2009**;113:6215-24

15. Isidori A, Cerchione C, Daver N, DiNardo C, Garcia-Manero G, Konopleva M*, et al.* Immunotherapy in Acute Myeloid Leukemia: Where We Stand. Front Oncol **2021**;11:656218
16. Haubner S, Perna F, Kohnke T, Schmidt C, Berman S, Augsberger C*, et al.* Coexpression profile of leukemic stem cell markers for combinatorial targeted therapy in AML. Leukemia **2019**;33:64-74
17. Daver N, Alotaibi AS, Bucklein V, Subklewe M. T-cell-based immunotherapy of acute myeloid leukemia: current concepts and future developments. Leukemia **2021**;35:1843-63
18. Cheng P, Chen X, Dalton R, Calescibetta A, So T, Gilvary D*, et al.* Immunodepletion of MDSC by AMV564, a novel bivalent, bispecific CD33/CD3 T cell engager, ex vivo in MDS and melanoma. Mol Ther **2022**;30:2315-26
19. Ravandi F, Stein AS, Kantarjian HM, Walter RB, Paschka P, Jongen-Lavrencic M*, et al.* A Phase 1 First-in-Human Study of AMG 330, an Anti-CD33 Bispecific T-Cell Engager (BiTE®) Antibody Construct, in Relapsed/Refractory Acute Myeloid Leukemia (R/R AML). Blood **2018**;132:25-
20. Subklewe M, Stein A, Walter RB, Bhatia R, Wei AH, Ritchie D*, et al.* Preliminary Results from a Phase 1 First-in-Human Study of AMG 673, a Novel Half-Life Extended (HLE) Anti-CD33/CD3 BiTE® (Bispecific T-Cell Engager) in Patients with Relapsed/Refractory (R/R) Acute Myeloid Leukemia (AML). Blood **2019**;134:833-
21. Westervelt P, Cortes JE, Altman JK, Long M, Oehler VG, Gojo I*, et al.* Phase 1 First-in-Human Trial of AMV564, a Bivalent Bispecific (2:2) CD33/CD3 T-Cell Engager, in Patients with Relapsed/Refractory Acute Myeloid Leukemia (AML). Blood **2019**;134:834-
22. Uy GL, Aldoss I, Foster MC, Sayre PH, Wieduwilt MJ, Advani AS*, et al.* Flotetuzumab as salvage immunotherapy for refractory acute myeloid leukemia. Blood **2021**;137:751-62
23. Uckun FM, Lin TL, Mims AS, Patel P, Lee C, Shahidzadeh A*, et al.* A Clinical Phase 1B Study of the CD3xCD123 Bispecific Antibody APVO436 in Patients with Relapsed/Refractory Acute Myeloid Leukemia or Myelodysplastic Syndrome. Cancers (Basel) **2021**;13
24. Boyiadzis M, Desai P, Daskalakis N, Donnellan W, Ferrante L, Goldberg JD*, et al.* First-in-human study of JNJ-63709178, a CD123/CD3 targeting antibody, in relapsed/refractory acute myeloid leukemia. Clin Transl Sci **2022**
25. Riether C, Pabst T, Hopner S, Bacher U, Hinterbrandner M, Banz Y*, et al.* Targeting CD70 with cusatuzumab eliminates acute myeloid leukemia stem cells in patients treated with hypomethylating agents. Nat Med **2020**;26:1459-67
26. Ehninger A, Kramer M, Rollig C, Thiede C, Bornhauser M, von Bonin M*, et al.* Distribution and levels of cell surface expression of CD33 and CD123 in acute myeloid leukemia. Blood Cancer J **2014**;4:e218
27. Perna F, Berman SH, Soni RK, Mansilla-Soto J, Eyquem J, Hamieh M*, et al.* Integrating Proteomics and Transcriptomics for Systematic Combinatorial Chimeric Antigen Receptor Therapy of AML. Cancer Cell **2017**;32:506-19 e5
28. Bowman MR, Crimmins MA, Yetz-Aldape J, Kriz R, Kelleher K, Herrmann S. The cloning of CD70 and its identification as the ligand for CD27. J Immunol **1994**;152:1756-61

29. Nolte MA, van Olffen RW, van Gisbergen KP, van Lier RA. Timing and tuning of CD27-CD70 interactions: the impact of signal strength in setting the balance between adaptive responses and immunopathology. Immunol Rev **2009**;229:216-31
30. Binz HK, Amstutz P, Kohl A, Stumpp MT, Briand C, Forrer P*, et al.* High-affinity binders selected from designed ankyrin repeat protein libraries. Nat Biotechnol **2004**;22:575-82
31. Rothenberger S, Hurdiss DL, Walser M, Malvezzi F, Mayor J, Ryter S*, et al.* The trispecific DARPin ensovibep inhibits diverse SARS-CoV-2 variants. Nat Biotechnol **2022**;40:1845-54
32. Zahnd C, Amstutz P, Pluckthun A. Ribosome display: selecting and evolving proteins in vitro that specifically bind to a target. Nat Methods **2007**;4:269-79
33. Kjer-Nielsen L, Dunstone MA, Kostenko L, Ely LK, Beddoe T, Mifsud NA*, et al.* Crystal structure of the human T cell receptor CD3 epsilon gamma heterodimer complexed to the therapeutic mAb OKT3. Proc Natl Acad Sci USA **2004**;101:7675-80
34. Campos-Lima PO, Levitsky V, Imreh MP, Gavioli R, Masucci MG. Epitope-dependent selection of highly restricted or diverse T cell receptor repertoires in response to persistent infection by Epstein-Barr virus. J Exp Med **1997**;186:83-9
35. Wei CH, Beeson C, Masucci MG, Levitsky V. A partially agonistic peptide acts as a selective inducer of apoptosis in CD8+ CTLs. J Immunol **1999**;163:2601-9
36. Zahnd C, Pecorari F, Straumann N, Wyler E, Pluckthun A. Selection and characterization of Her2 binding-designed ankyrin repeat proteins. J Biol Chem **2006**;281:35167-75
37. Binz HK, Stumpp MT, Forrer P, Amstutz P, Pluckthun A. Designing repeat proteins: well-expressed, soluble and stable proteins from combinatorial libraries of consensus ankyrin repeat proteins. J Mol Biol **2003**;332:489-503
38. Steiner D, Merz FW, Sonderegger I, Gulotti-Georgieva M, Villemagne D, Phillips DJ*, et al.* Half-life extension using serum albumin-binding DARPin(R) domains. Protein Eng Des Sel **2017**;30:583-91
39. Friedrich M, Henn A, Raum T, Bajtus M, Matthes K, Hendrich L*, et al.* Preclinical characterization of AMG 330, a CD3/CD33-bispecific T-cell-engaging antibody with potential for treatment of acute myelogenous leukemia. Mol Cancer Ther **2014**;13:1549-57
40. Reusch U, Harrington KH, Gudgeon CJ, Fucek I, Ellwanger K, Weichel M*, et al.* Characterization of CD33/CD3 Tetravalent Bispecific Tandem Diabodies (TandAbs) for the Treatment of Acute Myeloid Leukemia. Clin Cancer Res **2016**;22:5829-38
41. Chichili GR, Huang L, Li H, Burke S, He L, Tang Q*, et al.* A CD3xCD123 bispecific DART for redirecting host T cells to myelogenous leukemia: preclinical activity and safety in nonhuman primates. Sci Transl Med **2015**;7:289ra82
42. Johnson S, Burke S, Huang L, Gorlatov S, Li H, Wang W*, et al.* Effector cell recruitment with novel Fv-based dual-affinity re-targeting protein leads to potent tumor cytolysis and in vivo B-cell depletion. J Mol Biol **2010**;399:436-49
43. Alderson RF, Huang L, Zhang X, Li H, Kaufman T, Diedrich G*, et al.* Combinatorial Anti-Tumor Activity in Animal Models of a Novel CD123 x CD3 Bispecific Dart® Molecule (MGD024) with Cytarabine, Venetoclax or Azacitidine Supports Combination Therapy in Acute Myeloid Leukemia. Blood **2021**;138:1165-
44. Biedermann B, Gil D, Bowen DT, Crocker PR. Analysis of the CD33-related siglec family reveals that Siglec-9 is an endocytic receptor expressed on subsets of acute

myeloid leukemia cells and absent from normal hematopoietic progenitors. Leuk Res **2007**;31:211-20
45. Weber GF, Chousterman BG, He S, Fenn AM, Nairz M, Anzai A*, et al.* Interleukin-3 amplifies acute inflammation and is a potential therapeutic target in sepsis. Science **2015**;347:1260-5
46. Riether C, Schurch CM, Buhrer ED, Hinterbrandner M, Huguenin AL, Hoepner S*, et al.* CD70/CD27 signaling promotes blast stemness and is a viable therapeutic target in acute myeloid leukemia. J Exp Med **2017**;214:359-80
47. Liu W, Maben Z, Wang C, Lindquist KC, Li M, Rayannavar V*, et al.* Structural delineation and phase-dependent activation of the costimulatory CD27:CD70 complex. J Biol Chem **2021**;297:101102
48. Broughton SE, Hercus TR, Nero TL, Kan WL, Barry EF, Dottore M*, et al.* A dual role for the N-terminal domain of the IL-3 receptor in cell signalling. Nat Commun **2018**;9:386
49. Crocker PR, Paulson JC, Varki A. Siglecs and their roles in the immune system. Nat Rev Immunol **2007**;7:255-66
50. Fletcher EAK, Eltahir M, Lindqvist F, Rieth J, Tornqvist G, Leja-Jarblad J*, et al.* Extracorporeal human whole blood in motion, as a tool to predict first-infusion reactions and mechanism-of-action of immunotherapeutics. Int Immunopharmacol **2018**;54:1-11
51. Al-Hussaini M, Rettig MP, Ritchey JK, Karpova D, Uy GL, Eissenberg LG*, et al.* Targeting CD123 in acute myeloid leukemia using a T-cell-directed dual-affinity retargeting platform. Blood **2016**;127:122-31
52. Aigner M, Feulner J, Schaffer S, Kischel R, Kufer P, Schneider K*, et al.* T lymphocytes can be effectively recruited for ex vivo and in vivo lysis of AML blasts by a novel CD33/CD3-bispecific BiTE antibody construct. Leukemia **2013**;27:1107-15
53. Bennett TA, Montesinos P, Moscardo F, Martinez-Cuadron D, Martinez J, Sierra J*, et al.* Pharmacological profiles of acute myeloid leukemia treatments in patient samples by automated flow cytometry: a bridge to individualized medicine. Clin Lymphoma Myeloma Leuk **2014**;14:305-18
54. Wunderlich M, Brooks RA, Panchal R, Rhyasen GW, Danet-Desnoyers G, Mulloy JC. OKT3 prevents xenogeneic GVHD and allows reliable xenograft initiation from unfractionated human hematopoietic tissues. Blood **2014**;123:e134-44
55. Hu Y, Smyth GK. ELDA: extreme limiting dilution analysis for comparing depleted and enriched populations in stem cell and other assays. J Immunol Methods **2009**;347:70-8
56. Chou TC. Theoretical basis, experimental design, and computerized simulation of synergism and antagonism in drug combination studies. Pharmacol Rev **2006**;58:621-81
57. Chou TC. Drug combination studies and their synergy quantification using the Chou-Talalay method. Cancer Res **2010**;70:440-6
58. Chou TC, Martin N. CompuSyn for drug combinations: PC Software and User's Guide: a computer program for quantitation of synergism and antagonism in drug combinations, and the determination of IC50 and ED50 and LD50 values. ComboSyn **2005**
59. Vafa O, Trinklein ND. Perspective: Designing T-Cell Engagers With Better Therapeutic Windows. Front Oncol **2020**;10:446
60. Teachey DT, Lacey SF, Shaw PA, Melenhorst JJ, Maude SL, Frey N*, et al.* Identification of Predictive Biomarkers for Cytokine Release Syndrome after Chimeric Antigen

Receptor T-cell Therapy for Acute Lymphoblastic Leukemia. Cancer Discov **2016**;6:664-79
61. Harper T, Sharma A, Kaliyaperumal S, Fajardo F, Hsu K, Liu L*, et al.* Characterization of an Anti-CD70 Half-Life Extended Bispecific T Cell Engager (HLE-BiTE) and Associated On-Target Toxicity in Cynomolgus Monkeys. Toxicol Sci **2022**
62. Brugnoni D, Airo P, Marino R, Notarangelo LD, van Lier RA, Cattaneo R. CD70 expression on T-cell subpopulations: study of normal individuals and patients with chronic immune activation. Immunol Lett **1997**;55:99-104
63. Orengo AM, Cantoni C, Neglia F, Biassoni R, Ferrini S. Reciprocal expression of CD70 and of its receptor, CD27, in human long term-activated T and natural killer (NK) cells: inverse regulation by cytokines and role in induction of cytotoxicity. Clin Exp Immunol **1997**;107:608-13
64. Korpelainen EI, Gamble JR, Vadas MA, Lopez AF. IL-3 receptor expression, regulation and function in cells of the vasculature. Immunol Cell Biol **1996**;74:1-7
65. Sun Y, Wang S, Zhao L, Zhang B, Chen H. IFN-gamma and TNF-alpha aggravate endothelial damage caused by CD123-targeted CAR T cell. Onco Targets Ther **2019**;12:4907-25
66. Frankel AE, Woo JH, Ahn C, Pemmaraju N, Medeiros BC, Carraway HE*, et al.* Activity of SL-401, a targeted therapy directed to interleukin-3 receptor, in blastic plasmacytoid dendritic cell neoplasm patients. Blood **2014**;124:385-92
67. Pemmaraju N, Lane AA, Sweet KL, Stein AS, Vasu S, Blum W*, et al.* Tagraxofusp in Blastic Plasmacytoid Dendritic-Cell Neoplasm. N Engl J Med **2019**;380:1628-37
68. Castaigne S, Pautas C, Terre C, Raffoux E, Bordessoule D, Bastie JN*, et al.* Effect of gemtuzumab ozogamicin on survival of adult patients with de-novo acute myeloid leukaemia (ALFA-0701): a randomised, open-label, phase 3 study. Lancet **2012**;379:1508-16
69. Sallman DA, Elmariah H, Sweet K, Mishra A, Cox CA, Chakaith M*, et al.* Phase 1/1b Safety Study of Prgn-3006 Ultracar-T in Patients with Relapsed or Refractory CD33-Positive Acute Myeloid Leukemia and Higher Risk Myelodysplastic Syndromes. Blood **2022**;140:10313-5
70. Sallman DA, DeAngelo DJ, Pemmaraju N, Dinner S, Gill S, Olin RL*, et al.* Ameli-01: A Phase I Trial of UCART123v1.2, an Anti-CD123 Allogeneic CAR-T Cell Product, in Adult Patients with Relapsed or Refractory (R/R) CD123+ Acute Myeloid Leukemia (AML). Blood **2022**;140:2371-3
71. Jin X, Zhang M, Sun R, Lyu H, Xiao X, Zhang X*, et al.* First-in-human phase I study of CLL-1 CAR-T cells in adults with relapsed/refractory acute myeloid leukemia. J Hematol Oncol **2022**;15:88
72. Goswami M, Hourigan CS. Novel Antigen Targets for Immunotherapy of Acute Myeloid Leukemia. Curr Drug Targets **2017**;18:296-303
73. Sami SA, Darwish NHE, Barile ANM, Mousa SA. Current and Future Molecular Targets for Acute Myeloid Leukemia Therapy. Curr Treat Options Oncol **2020**;21:3
74. Laszlo GS, Beddoe ME, Godwin CD, Bates OM, Gudgeon CJ, Harrington KH*, et al.* Relationship between CD33 expression, splicing polymorphism, and in vitro cytotoxicity of gemtuzumab ozogamicin and the CD33/CD3 BiTE(R) AMG 330. Haematologica **2019**;104:e59-e62
75. Ravandi F, Walter RB, Subklewe M, Buecklein V, Jongen-Lavrencic M, Paschka P*, et al.* Updated results from phase I dose-escalation study of AMG 330, a bispecific T-cell

engager molecule, in patients with relapsed/refractory acute myeloid leukemia (R/R AML). Journal of Clinical Oncology **2020**;38:7508-

Tables

Table 1. Kinetic parameters of MP0533 to human recombinant targets by SPR

Protein name	k_{on} [$M^{-1}s^{-1}$]	k_{off} [s^{-1}]	K_d [M]	Rmax [RU]	Chi^2/Rmax [%]
HSA	9.3E+04	1.1E-02	1.2E-07	103.4	4.7
hCD33	9.6E+05	4.9E-03	5.1E-09	148.5	23.1
hCD123	6.9E+05	3.9E-05	5.6E-11	119.2	0.8*
hCD70	7.6E+04	4.7E-05	6.1E-10	69.6	14.4
hCD3	1.4E+05	3.4E-03	2.4E-08	50.6	10.6

*Value is calculated using Chi^2/ndof (given readout on Sierra Analyzer) instead of Chi^2 (standard readout) - (ndof=number of degrees of freedom)

h, human; HSA, human serum albumin

Figure Legends

Figure 1. MP0533 induces potent killing of AML cell lines. (A) The six domains of the MP0533 molecule from N- to C-terminus: two HSA-binding domains (grey), CD33-binding domain (yellow), CD123-binding domain (orange), CD70-binding domain (green), CD3-binding domain (blue). **(B)** MP0533-induced T-cell activation and tumor cell killing in co-cultures with MOLM-13 cell lines expressing different TAA combinations (as indicated in the legend). **(C)** Tumor cell killing of different AML cell lines with corresponding EC50s. A representative experiment in duplicate ± SD is shown. **(D)** Tumor cell killing vs. cytokine release induced by MP0533 and comparator TCEs. The average of MOLM-13 and RPMI8226 killing assays ± SD is shown. For all panels, T-cell activation and tumor cell killing were assessed by flow cytometry by upregulation of CD25 on CD8 T cells and by cell count of remaining living cells, respectively, after 48 h co-incubation of T cell and tumor cells at E:T of 5:1. Control molecules shown: NB-CD3 DARPin (non-TAA binding) and TAA-NB DARPin (non-CD3 binding). Other TCEs shown: CD33-CD3 Bivalent (based on AMV564 sequence), CD33-CD3 BiTE (based on AMG330 sequence), CD123-CD3 DART (based on flotetuzumab sequence), HLE-CD123-CD3 DART, and CD123-CD3 ADAPTIR (based on APVO436 sequence).

Figure 2. MP0533 efficacy and safety profile in hPBMC mouse model xenografted subcutaneously with MOLM-13 cells. (A) Study design. **(B)** Tumor growth over time in mice injected intraperitoneally with hPBMC (n=5 mice per donor, 2 to 6 hPBMC donors used), xenografted subcutaneously with MOLM-13 cells. Mice randomization was based on MOLM-13 tumor size and hPBMC donors. Therapeutic treatments were initiated eight days after tumor cell injection, when the average tumor volume was around 150 mm^3. MP0533 and control DARPins (NB-CD3 DARPin = non-TAA binding and TAA-NB DARPin = non-CD3 binding) were administrated intravenously (i.v.) three times per week for 2 weeks, while CD33-CD3 BiTE and CD123-CD3 DART were administrated i.v. daily (as not half-life extended) for 2 weeks. Data are presented as mean ± SEM. **(C)** Three days after the first treatment, some mice were sacrificed for *ex vivo* analysis. Tumors were dissociated and analyzed by flow cytometry, and data are shown as % of activated T cells (CD8+CD25+CD69+) in the tumors. Release of cytokines was measured in the blood **(D)** and in the tumors **(E)** 4 h and 3 days after first treatment, respectively. Lines in **C-E** represent median values.

Figure 3. MP0533 efficacy and safety profile in hPBMC mouse model xenografted intravenously with MOLM-13 cells. (A) Study design. **(B-C)** Tumor growth over time in mice injected intraperitoneally (i.p.) with hPBMC (n=5 mice per donor, 2 hPBMC donors used, n=10 mice per group), xenografted intravenously (i.v.) with MOLM-13 LUC cells. Mice were treated with vehicle, serial dilutions of MP0533, or CD123-CD3 DART at 0.5 mg/kg starting five days after tumor cell injection. MP0533 was administrated i.v. three times per week for 2 weeks, while CD123-CD3 DART was administrated i.v. daily (as not half-life extended) for 2 weeks (no treatment was administered anymore after day 19 post-engraftment). Mouse randomization was based on imaging (photons/sec) at day 4 after tumor injection. Bioluminescence was then measured every 3-4 days using a Newton 7.0 device 10 min after i.p. injection of 150 mg/kg of D-luciferin and is plotted as photons/sec. Data in **(B)** are presented as mean ± SEM, while in **(C)** single mouse data are shown. **(D)** Representative pictures of MOLM-13 LUC-engrafted mice at day 21 after treatment initiation, 10 min exposure. **(E)** Release of cytokines was measured in the blood 4 h after first treatment. Single values and median are shown, with open vs. filled symbols indicating PBMCs from two

different donors. Samples under the lower limit of detection were assigned an arbitrary value below the assay range, indicated with the dotted line. Statistical significance was calculated by one-way ANOVA, Dunnett's multiple comparisons test: ****P<0.0001; ***P<0.001; ns, not significant.

Figure 4. MP0533 induces low cytokine release in whole blood. (A) Cytokine release and **(B)** cell counts in healthy donor (HD) whole blood loops after 0-24 h incubation and are shown as AUC overtime (0-4-8-24 h), average ± SD of 6 HD over 2 independent studies. Additional cytokine release in HD whole blood was measured in a 96-well plate format after 24 h incubation without **(C)** or after 6 h incubation with **(D)** MOLM-13 spiked into the blood to simulate a blast content of about 20%. Open symbols in **(D)** indicate whole blood without MOLM-13 cells, only assessed at 10 nM (shown off axis for clarity). Average ± SD of 3 and 2 HD is shown for **(C)** and **(D)**, respectively. For all panels, quantification of cytokines was performed by MSD MULTI-ARRAY technology. Hematology parameters in **(B)** were automatically measured by a Sysmex Hematology Analyzer instrument. Control molecules shown: NB-CD3 DARPin (non-TAA binding) and TAA-NB DARPin (non-CD3 binding). Other TCEs shown: CD33-CD3 BiTE (based on AMG330 sequence) and CD123-CD3 DART (based on flotetuzumab sequence).

Figure 5. Safety profile of MP0533 on healthy cells. (A) MP0533-induced T-cell activation and killing of basophils were assessed by flow cytometry by upregulation of CD25 on CD4 (left panel) and CD8 (middle panel) T cells, and by cell count of remaining living basophils (right panel) after 48 h co-incubation of autologous T cell and basophils at E:T of 4:1. **(B)** Viability (left panels) and proliferation (right panels) of CD4 and CD8 T cells after 5 days co-culture with MOLM-13 cells at E:T of 5:1. **(C)** Killing of CD123+ HUVEC was followed overtime with IncuCyte. HUVEC were first stimulated with TNFα and IFNγ (low = 0.3 ng/ml TNFα and 1 ng/ml IFNɣ; high = 10 ng/ml each) to induce expression of CD123, and then co-incubated with allogeneic pan T cells for 2 days at E:T of 5:1. Killing of HUVEC is shown as ratio of AUC ± SD of Annexin V green (dead HUVEC)/Cytolight red (living HUVEC) overtime. For all panels, the average ± SD of experiments using T cells and/or basophils from 2 different donors is shown. Control molecules shown: NB-CD3 DARPin (non-TAA binding) and TAA-NB DARPin (non-CD3 binding). Other TCEs shown: CD33-CD3 BiTE (based on AMG330 sequence), CD123-CD3 DART (based on flotetuzumab sequence), and CD123-CD3 ADAPTIR (based on APVO436 sequence).

Figure 6. MP0533 induces potent killing of primary AML cells and LSCs. (A) T-cell activation (left panel), proliferation (right panel, black curves), and tumor cell killing (right panel, red curves) were assessed on primary autologous whole bone marrow samples from 5 AML donors. The percentage of $CD25^+$ total T cells ± SD (left panel) and median curve fits (right panel) after 48 h and 120 h are shown. **(B)** LSC or HSC killing and colony forming assay (left panel) and TAA expression (right panel). CD45int/Lin-/CD90-/CD34+ cells were sorted from AML or HD PBMC or BMMC samples and TAA expression measured by flow cytometry and shown as ΔMFI over isotype control. Cell killing was assessed after 4 days co-incubation with allogeneic T cells from healthy donors at E:T of 1:1 followed by 14 days colony culture in semi-solid medium. Median of ΔMFI and percentage (of vehicle) colony count ± SEM are shown (from 5 AML samples and 4 HD samples). Control molecules shown: NB-CD3 DARPin (non-TAA binding) and CD70-CD3 DARPin (CD70 single-targeting TCE DARPin). Other TCEs shown: CD33-CD3 BiTE (based on AMG330 sequence) and CD123-CD3 DART (based on

flotetuzumab sequence). **(C)** Killing of LSCs in two AML PDX samples was assessed *in vivo* after 2 days *ex vivo* co-culture with allogeneic T cells at E:T of 1:1 and 10 pM MP0533 or control. Serial dilutions of treated cells were then injected into irradiated NSG mice and engraftment determined by the presence of hCD45+CD33+ in the bone marrow (left panel). Additionally, presence of LSCs in bone marrow of engrafted mice was confirmed *ex vivo* by 14 days colony culture in semi-solid medium (right panel). LSC frequencies were estimated with the ELDA software (http://bioinf.wehi.edu.au/software/elda/) and significant differences in LSC frequencies were calculated by chi-squared test (for PDX1: NB-CD3 vs. MP0533: P = 0.026; NB-CD3 vs. CD123-CD3 DART: P = 1.36×10^{-4}; MP0533 vs. CD123-CD3 DART: P = 0.105. For PDX2: NB-CD3 vs. MP0533: P = 0.011; NB-CD3 vs. CD123-CD3 DART: P = 0.011; MP0533 vs. CD123-CD3 DART: P = 1). Data from PDX1 (circles) and PDX2 (squares) engrafted mice are shown individually and as mean ± SD.

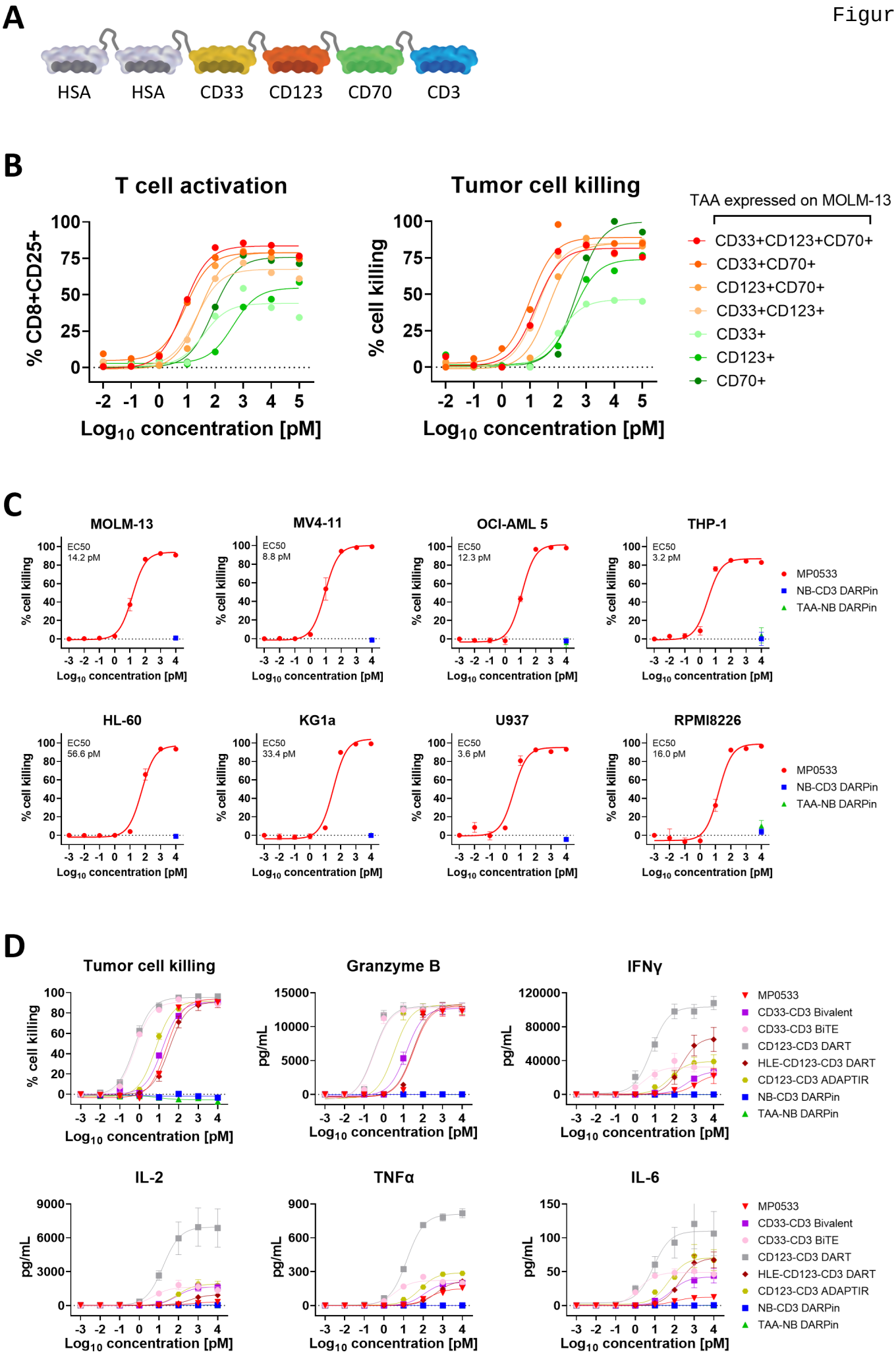

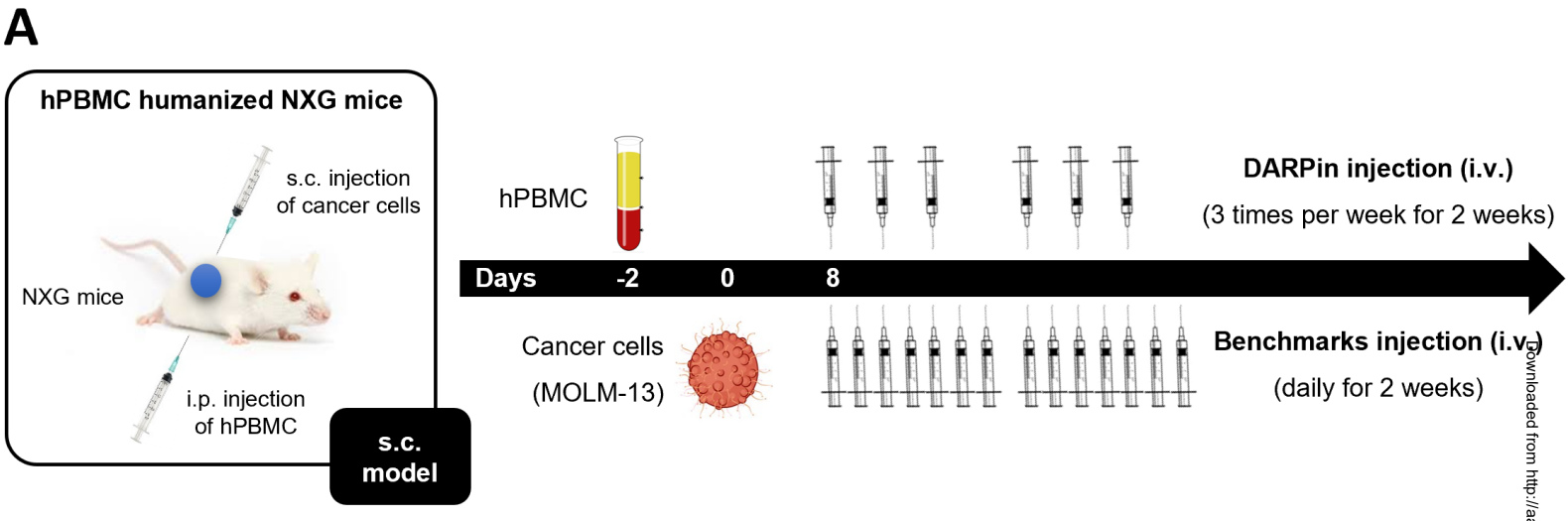

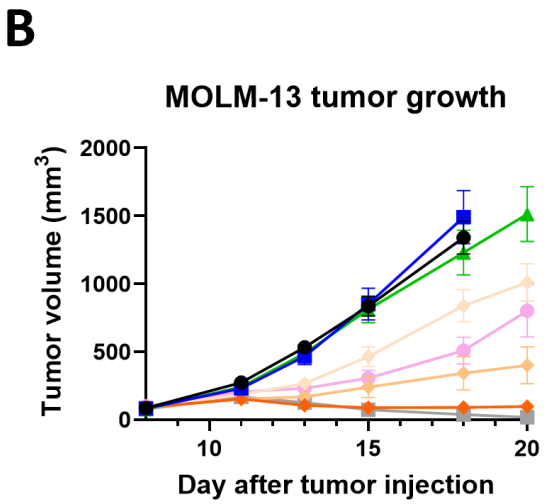

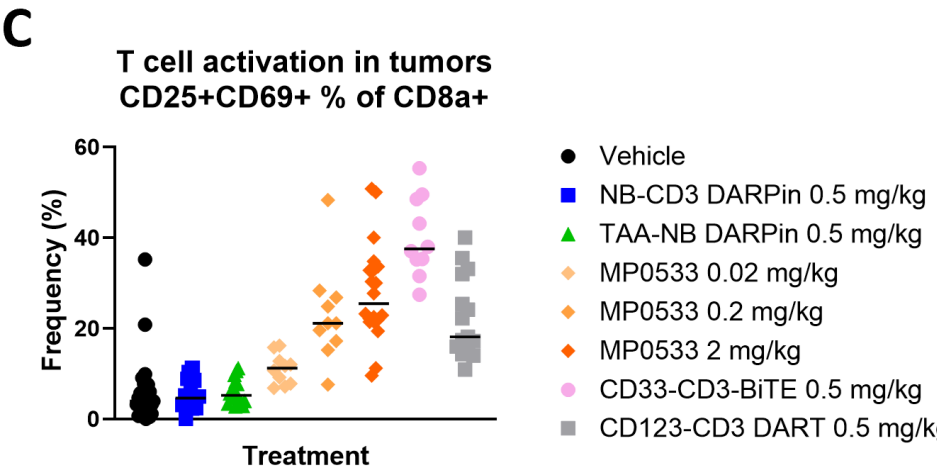

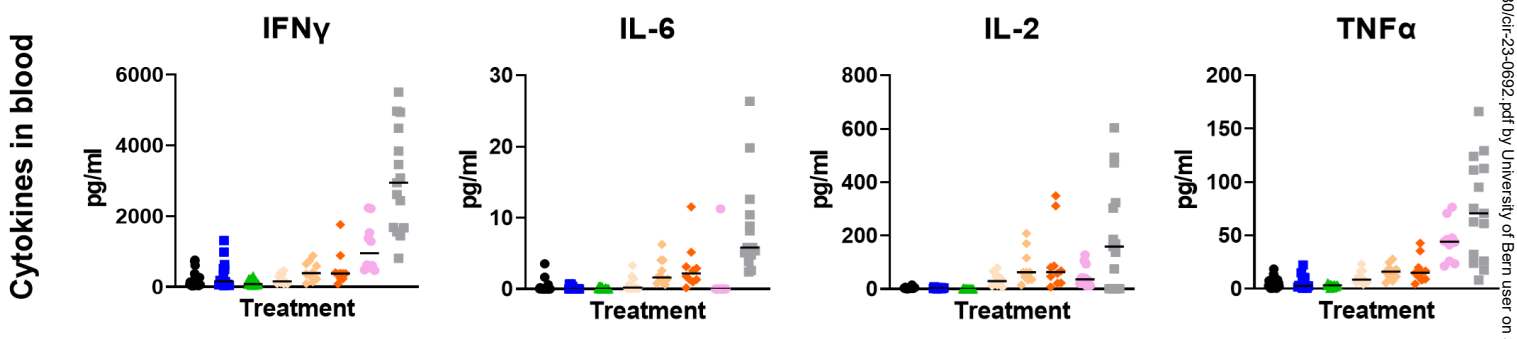

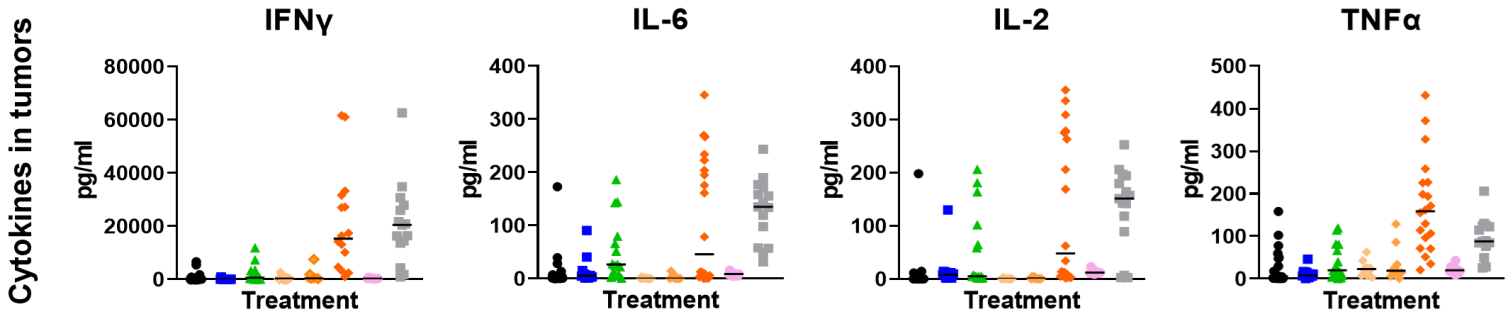

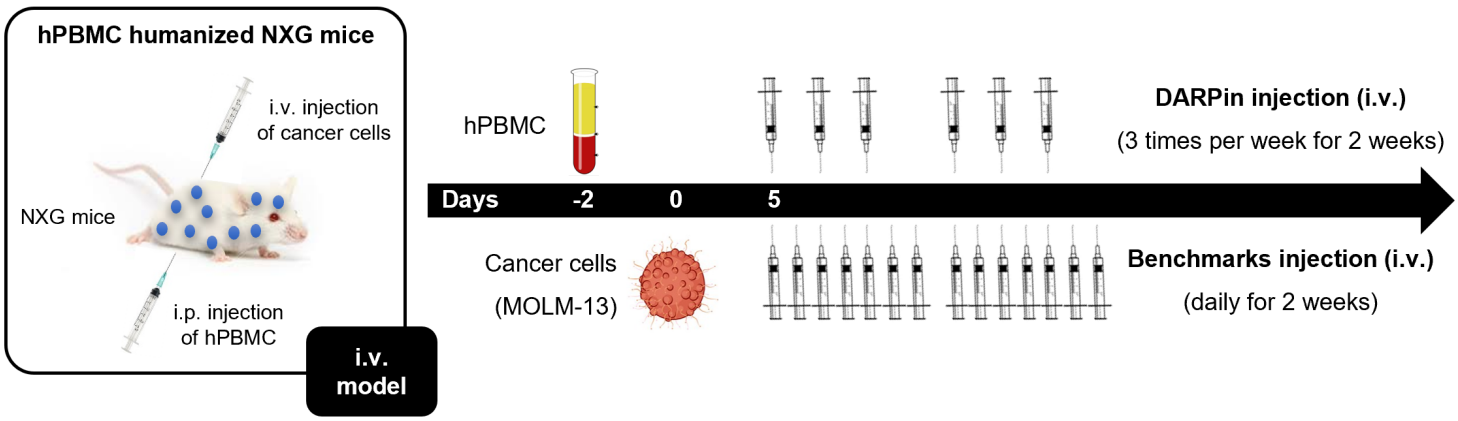

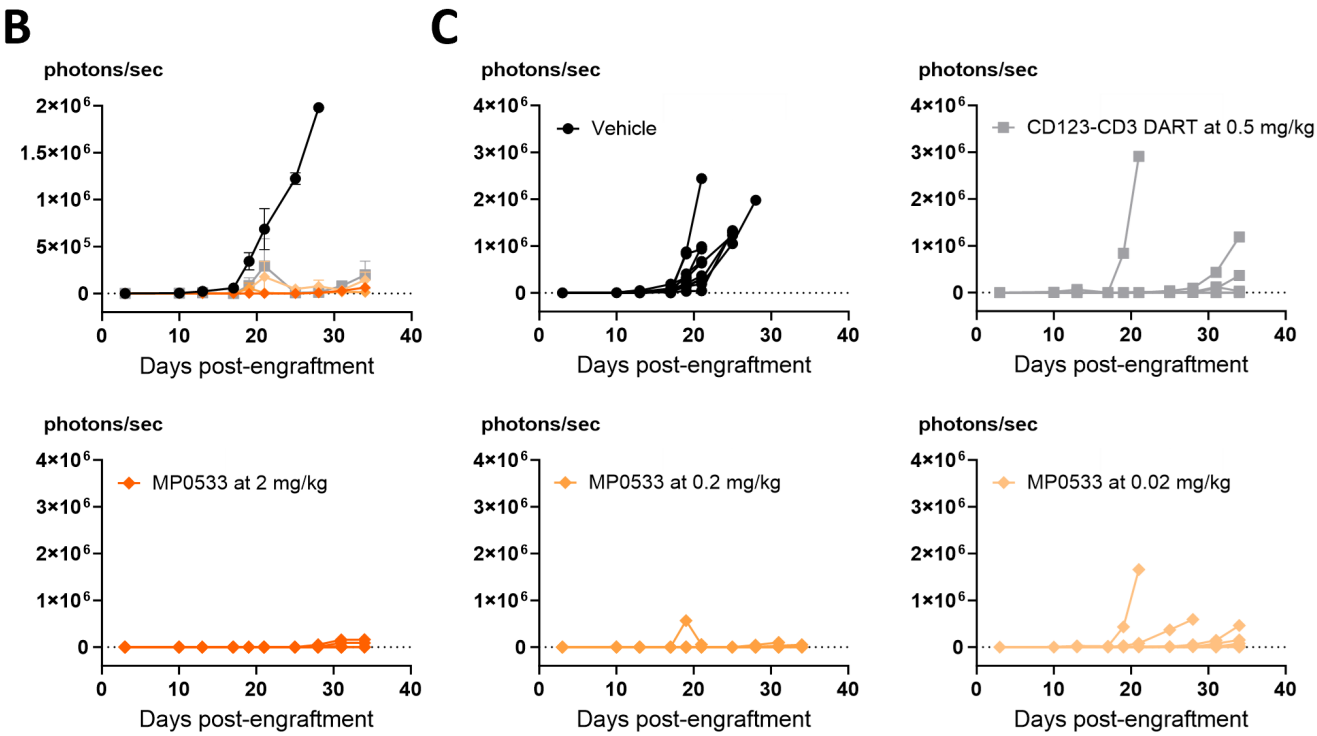

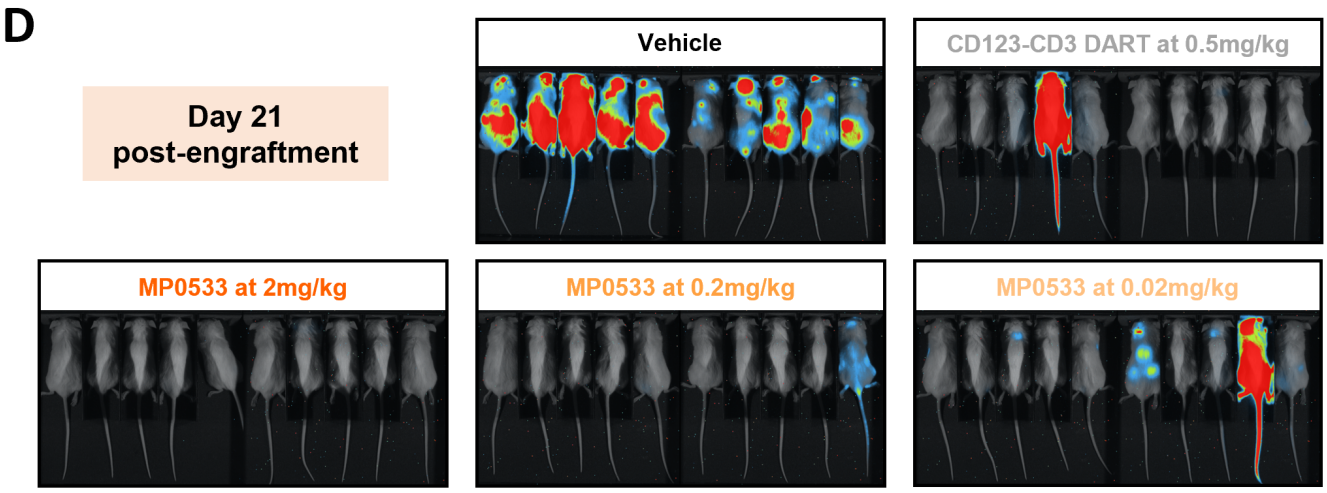

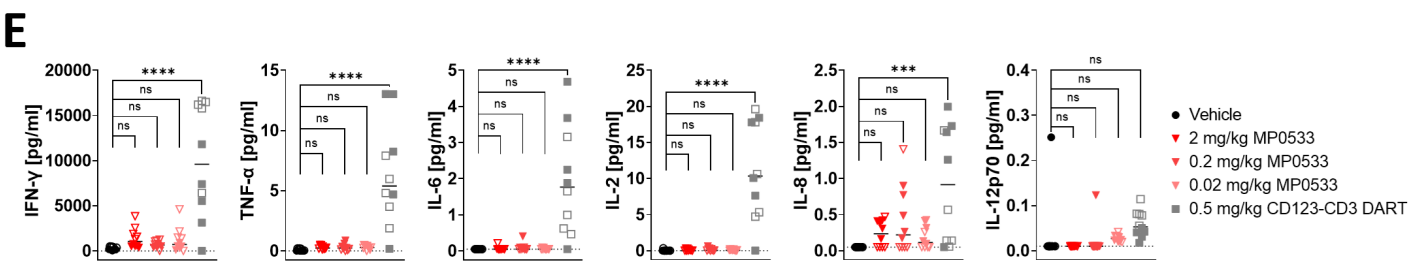

Figure 4

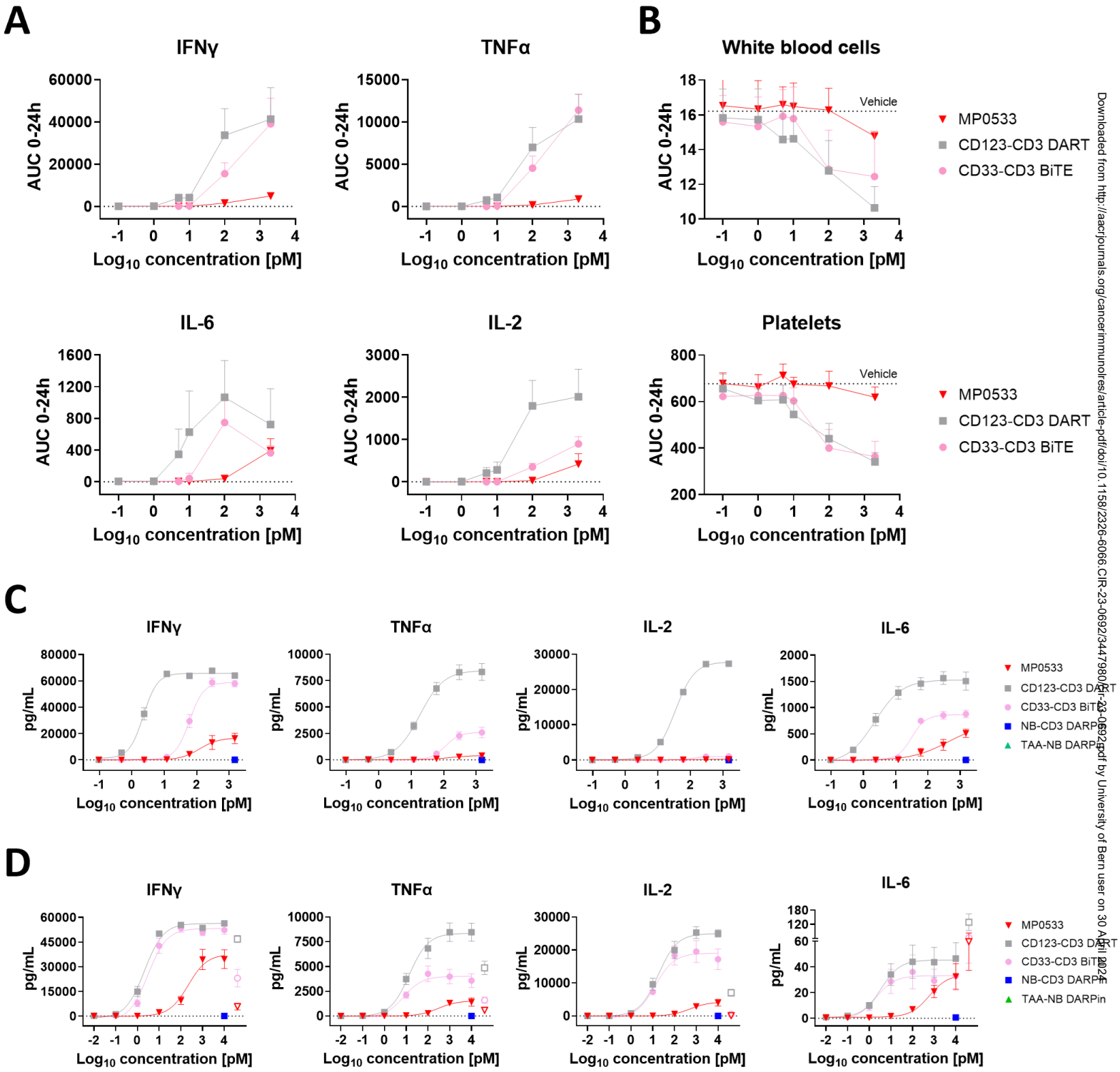

Figure 5